Production of π^+ and K^+ mesons in 3.2 AGeV argon-nucleus interactions at the Nuclotron

M.Kapishin, L.Kovachev, V.Plotnikov, Yu.Petukhov, I.Rufanov, M.Zavertyaev, A.Zinchenko

VBLHEP, JINR, Dubna, Russia

Joint Institute for Nuclear Research

SCIENCE BRINGING NATIONS TOGETHER

BM@N
collaboration meeting
14.09.2022

Outline

1. Run with argon beam (March 2018)
   - ✓ BM@N detector set-up
2. Data analysis (*Ar+C*, *Ar+Al*, *Ar+Cu*, *Ar+Sn*, *Ar+Pb* at 3.2A GeV)
   - ✓ Selection criteria
   - ✓ Reconstructed signal of π^+/K^+ (dN/dY & dN/p_T spectra)
   - ✓ Data - MC agreement: multiplicity, momentum spectra
   - ✓ Decomposition of π^+/K^+ reconstruction efficiency
   - ✓ Trigger, luminosity and mean impact parameters
   - ✓ Cross section and yields of π^+/K$^+$
   - ✓ Reconstructed p_T spectra of π^+/K$^+$ and extracted inverse slope parameter
   - ✓ Systematic uncertainty and extrapolation factors
3. Summary and plans

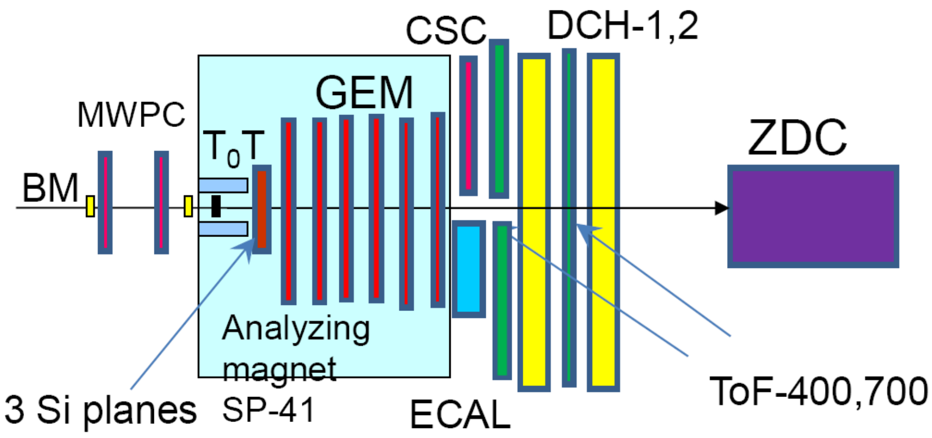

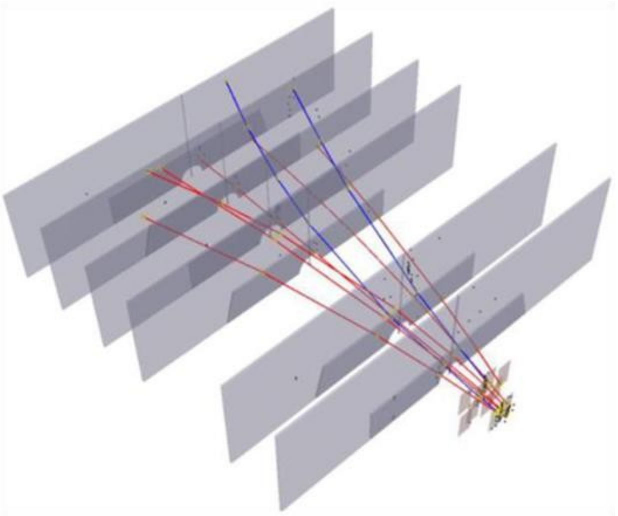

Central tracker in argon run.

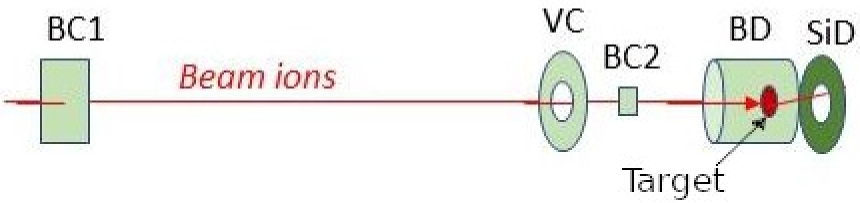

Schematic view of the beam counters, barrel detector, forward silicon detector and target.

Event selection criteria

- ✓ Beam halo, pile-up suppression within the readout time window, number of signals in the start detector: BC1=1, number of signals in the beam counter: BC2=1, number of signals in the veto counter around the beam: Veto=0;

Trigger condition in the multiplicity and barrel detectors: number of signals FD≥n, n ∈ [2;4], BD≥m, m ∈ [2;4] and combinations of FD and BD triggers (run dependent).

Table 1. Number of triggered events, beam fluxes and integrated luminosities collected for the argon beam of 3.2A GeV (*ToF-400* (*ToF-700*)).

Interactions (target thickness)	**Number of triggers / 10^6**	**Integrated beam flux / 10^7**	**Integrated luminosity / 10^{30} cm^{-2}**
Ar+C (2mm)	11.7 (11.3)	10.9 (8.7)	2.06 (1.97)
Ar+Al (3.33mm)	30.6 (29.2)	15.4 (10.2)	2.30 (2.05)
Ar+Cu (1.67mm)	30.9 (28.7)	15.9 (11.3)	1.79 (1.60)
Ar+Sn (2.57mm)	30.0 (25.9)	15.1 (9.5)	1.11 (0.91)
Ar+Pb (2.5mm)	13.7 (13.7)	7.0 (4.9)	0.50 (0.40)

π^+ and K^+ selection criteria

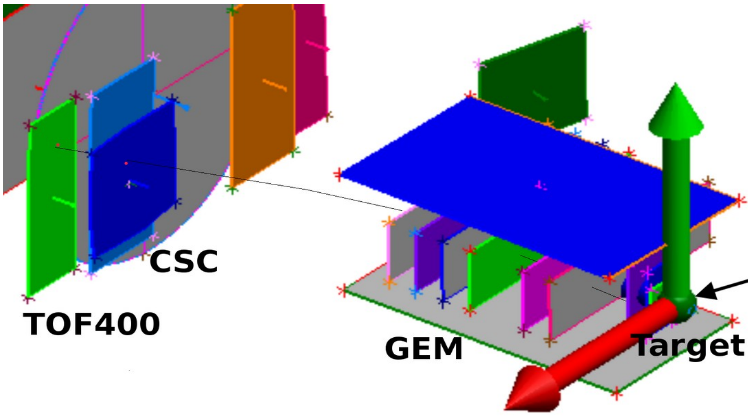

Abbreviation:

- ✓ PV – primary vertex

- ✓ Number of hits in 6 GEM per track > 3
- ✓ Tracks from PV: $-3.4 < Z_{PV} - Z_0 < 1.7$ cm
- ✓ Momentum range of tracks for ToF-400 (ToF-700): $p <$ 0.5 (0.7) GeV/c
- ✓ Distance from a track to PV in the X-Y plane: $dca < 1$ cm
- ✓ χ^2/ndf for tracks from the PV $< 3.5^2$
- ✓ Distance of extrapolated tracks to *CSC* (*DCH*) and *ToF-400* (*ToF-700*): $|resid_{X,Y}| < 2.5\ \sigma$ of hit-track residual distribution

Table2. Reconstructed signals of π^+ and K^+ for *ToF-400* and *ToF-700*.

Particle, Detector	Target				
	C	*Al*	*Cu*	*Sn*	*Pb*
π^+, *ToF-400*	4020±66	21130±152	28010±175	32060±186	22420±156
π^+, *ToF-700*	1070±34	5640±80	8090±95	9450±104	6830±86
K^+, *ToF-400*	45±10	278±25	538±31	729±36	570±32
K^+, *ToF-700*	31±6	117±16	193±21	346±23	221±20

Signal of π^+ in *Ar+Sn* interaction

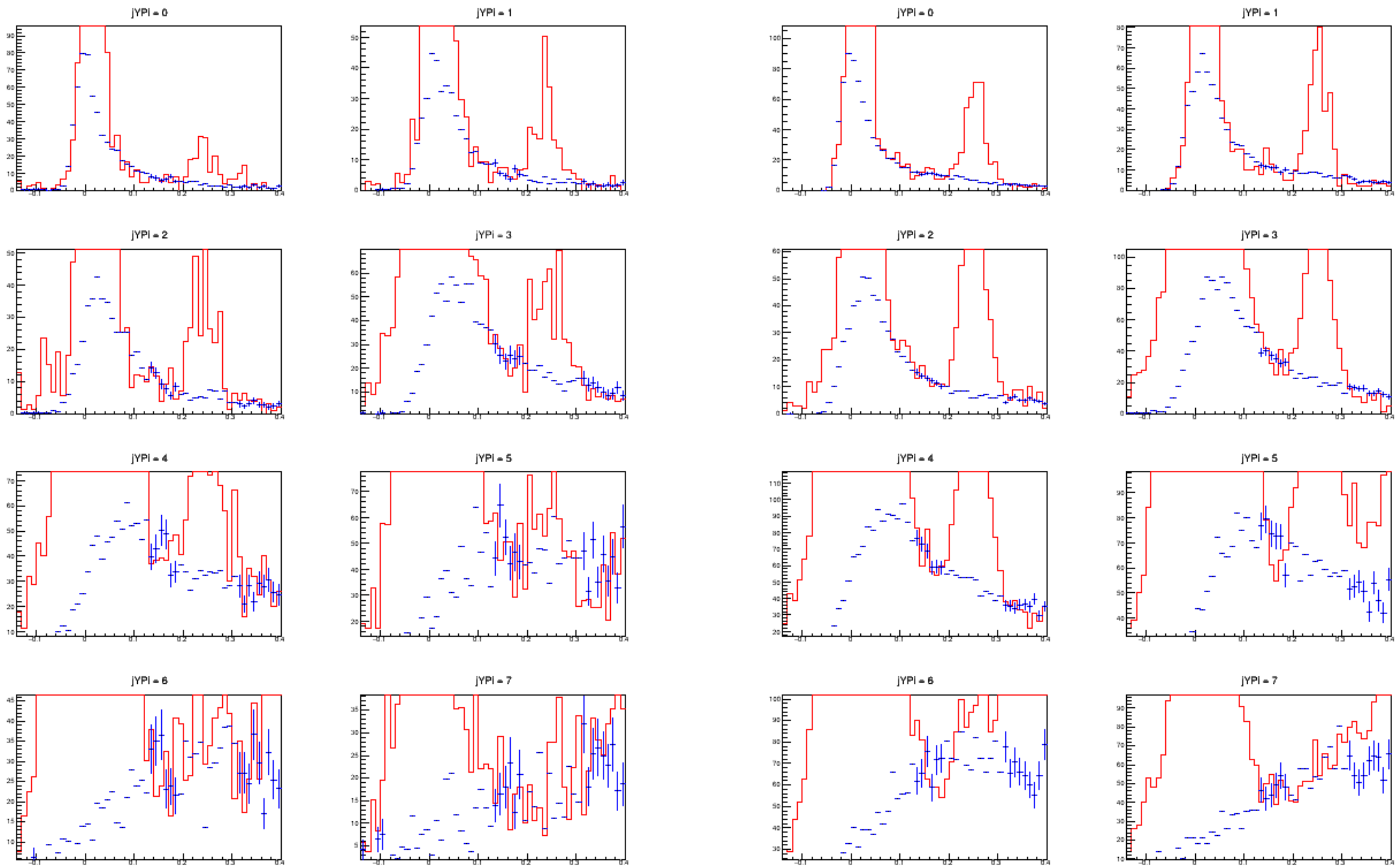

Fig. 10e. Spectrum of mass squared in bins of *y* of π^+ identified in *ToF-400* in *Ar+Sn* interactions at 3.2 AGeV argon beam energy: left) experimental events, right) simulated events. Background (blue histogram) subtraction by mixed events.

Signal of K^+ in $Ar+Sn$ interaction

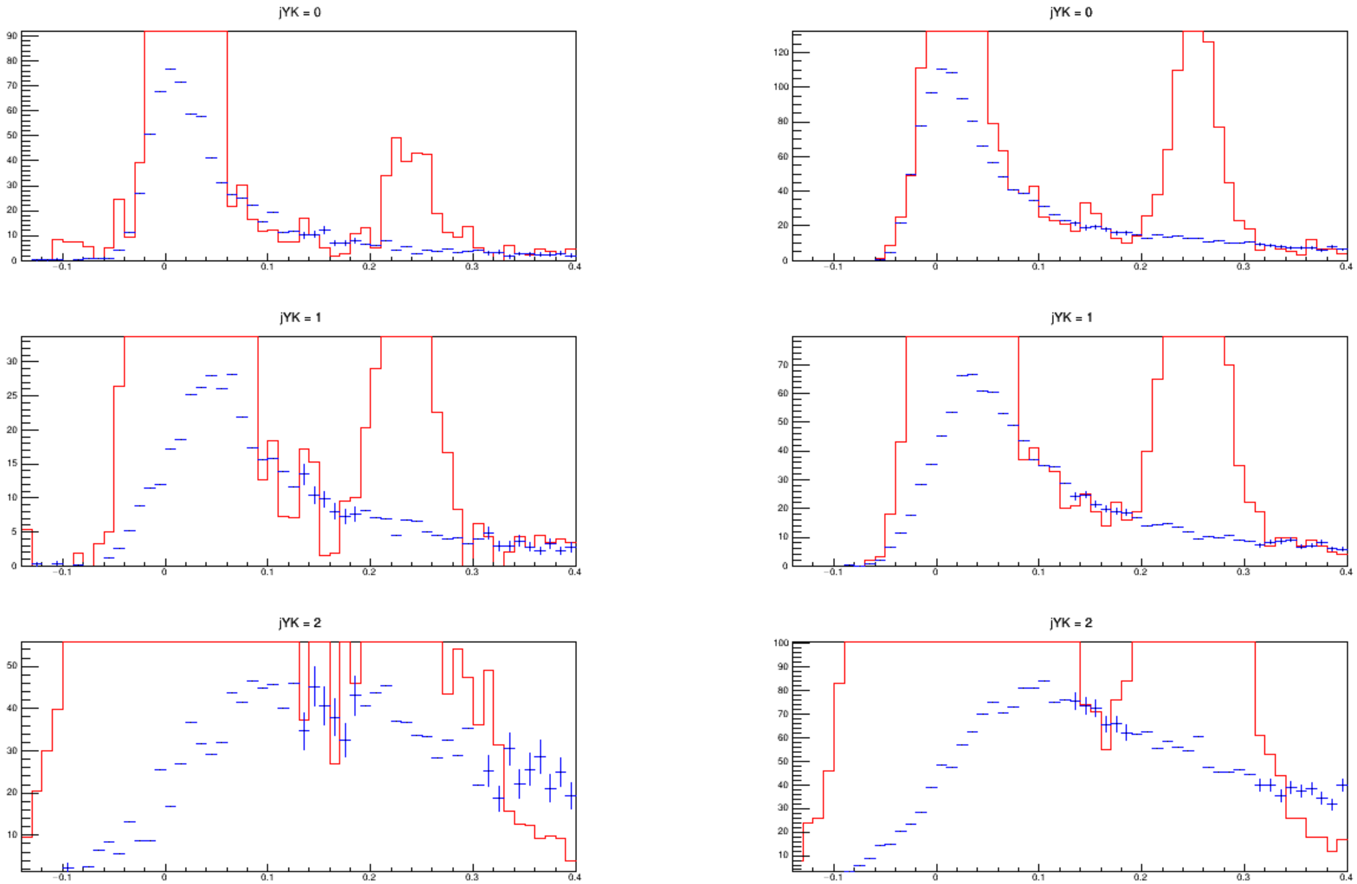

Fig. 10f. Spectrum of mass squared in bins of *y* of K^+ identified in *ToF-400* in *Ar+Sn* interactions at 3.2 AGeV argon beam energy: left) experimental events, right) simulated events. Background (blue histogram) is taken from mixed events and normalized to the red signal histogram in the mass squared range below and above the K^+ peak.

Signal of π^+ in *Ar+Cu* interaction

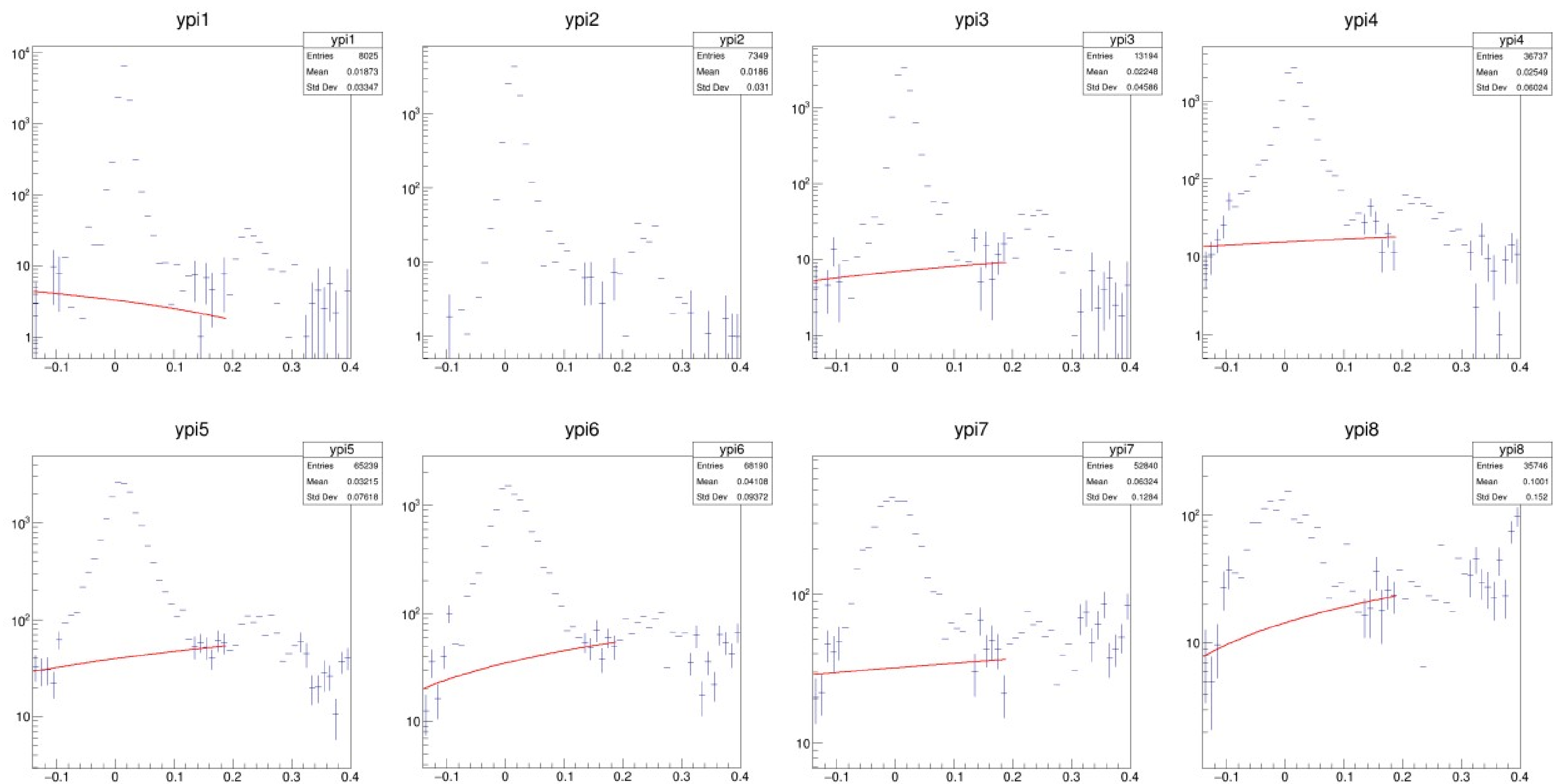

Fig. 10c. Spectrum of mass squared in bins of y of π^+ identified in *ToF-400* in *Ar+Cu* interactions: background subtraction by the linear fit.

Signal of K^+ in $Ar+Cu$ interaction

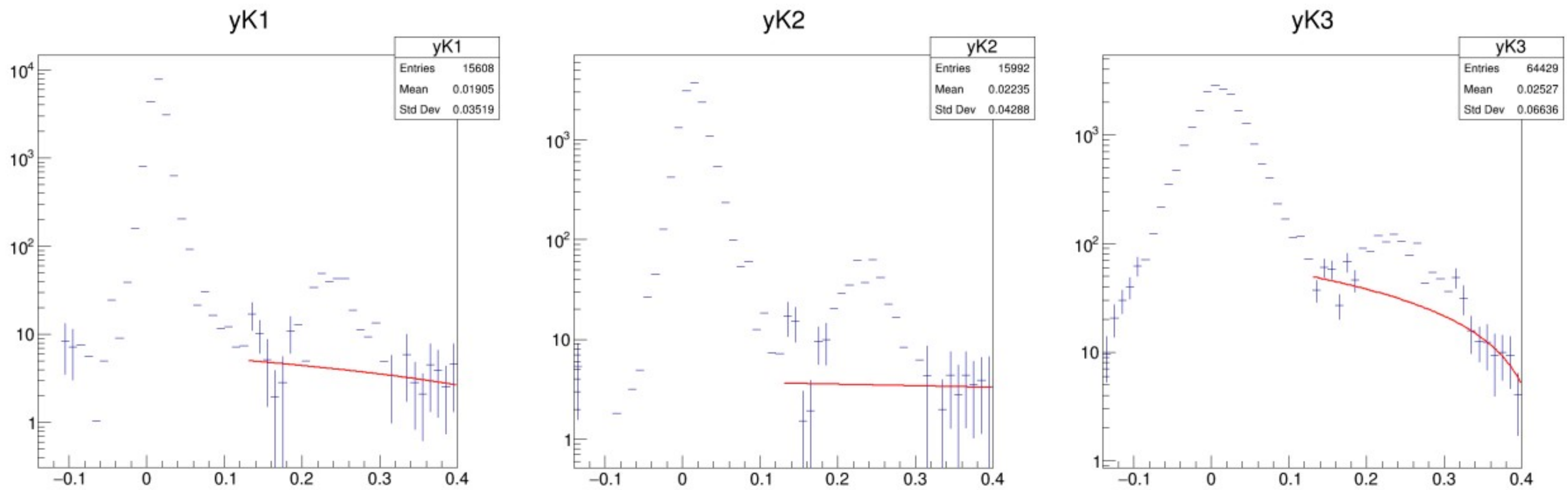

Fig. 10d. Spectrum of mass squared in bins of y of K^+ identified in *ToF-400* in *Ar+Cu* interactions: background subtraction by the linear fit.

Comparison of experimental data and MC

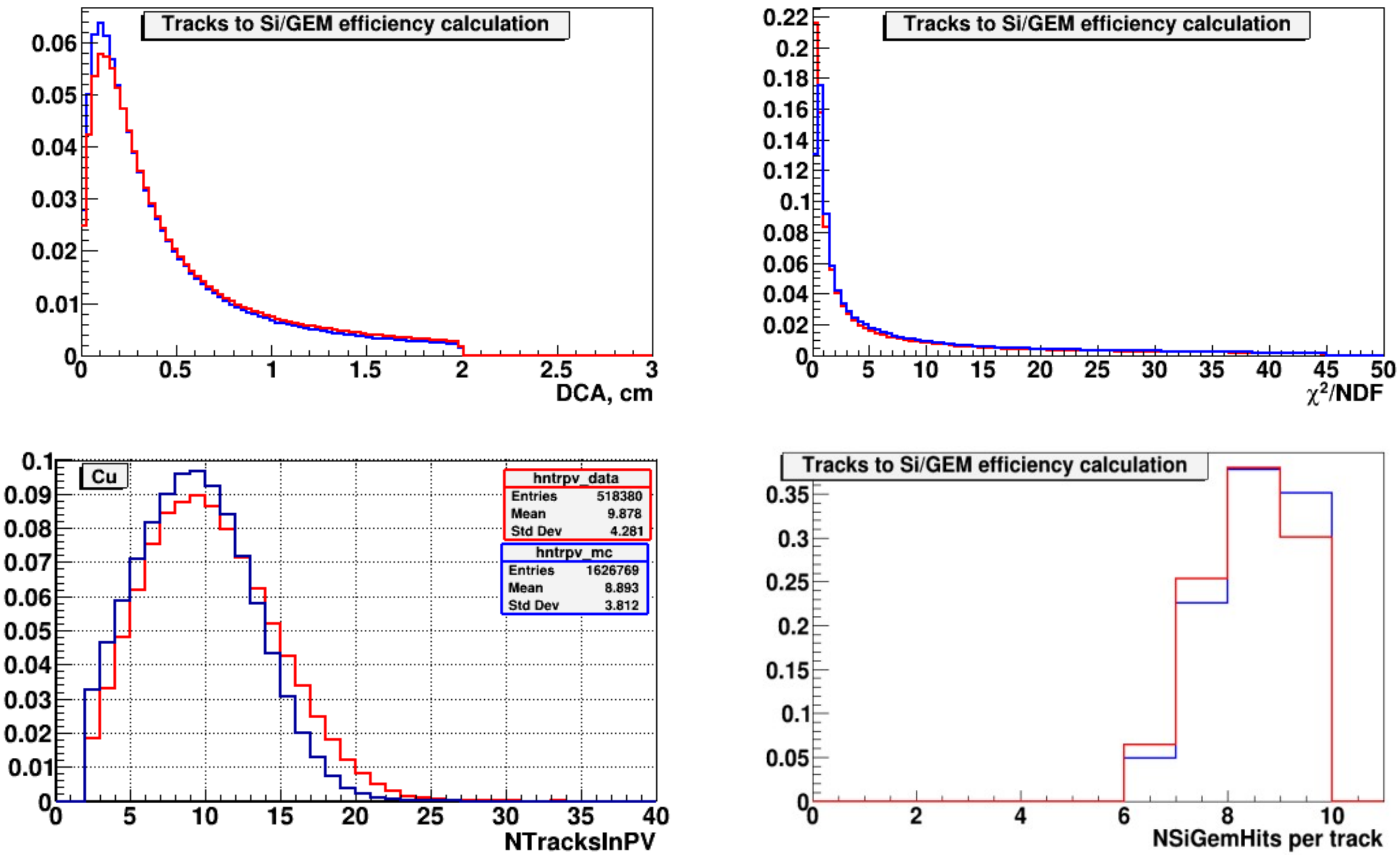

Fig. 3a. *Ar+A* interactions at 3.2 AGeV argon beam energy: comparison of experimental distributions (red lines) and Monte Carlo GEANT distributions of events generated with the DCM-SMM model (blue lines): Distribution of the distance of the closest approach DCA between tracks and the vertex in the plane perpendicular to the beam direction; χ^2 of reconstructed tracks; number of tracks reconstructed in the primary vertex; number of hits per track reconstructed in 3 Si + 6 GEM detectors.

Comparison of experimental data and MC

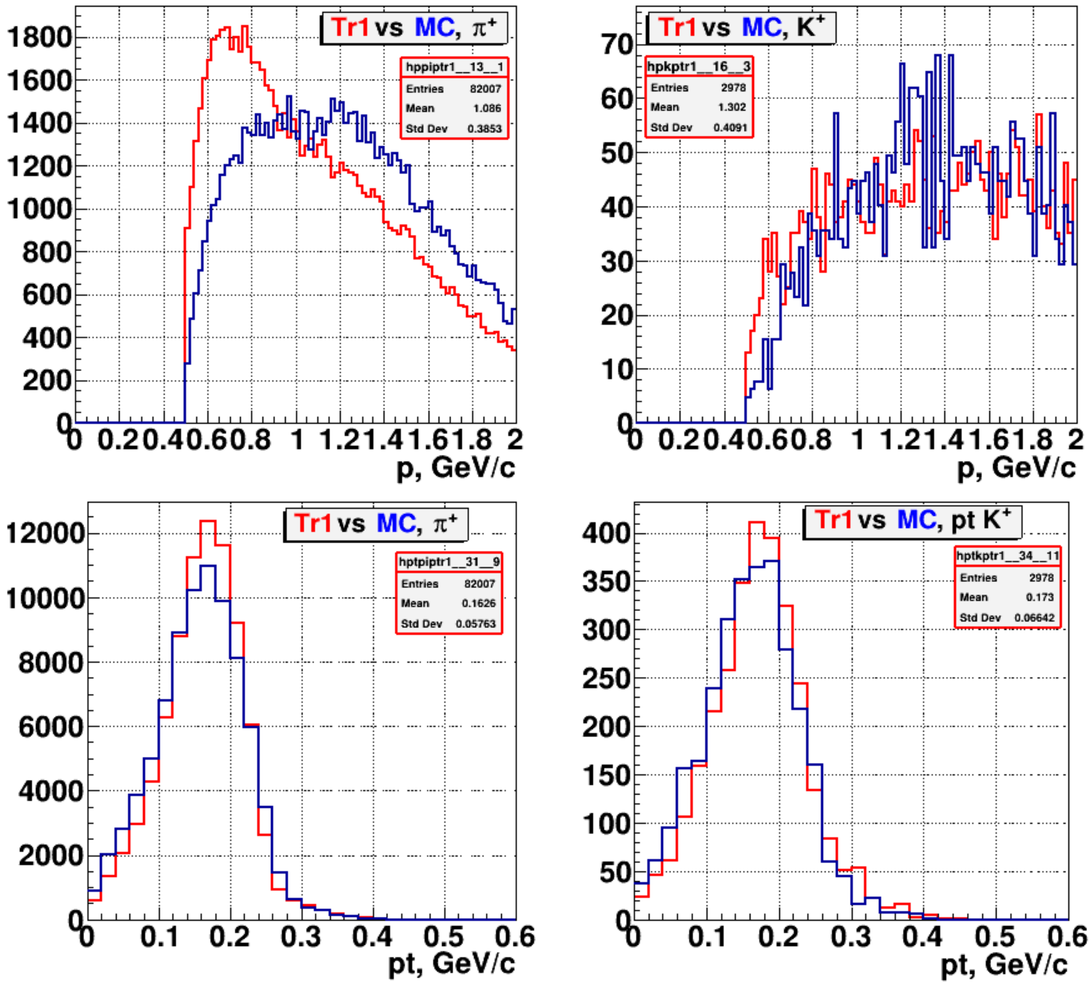

Fig. 3b. *Ar+A* interactions at 3.2 AGeV argon beam energy: comparison of *ToF-400* experimental data (red curves) and DCM-SMM + GEANT Monte Carlo simulation (blue curves): total momentum of identified π^+ and K^+ (upper plots); transverse momentum of π^+ and K^+ (lower plots).

Comparison of experimental data and MC

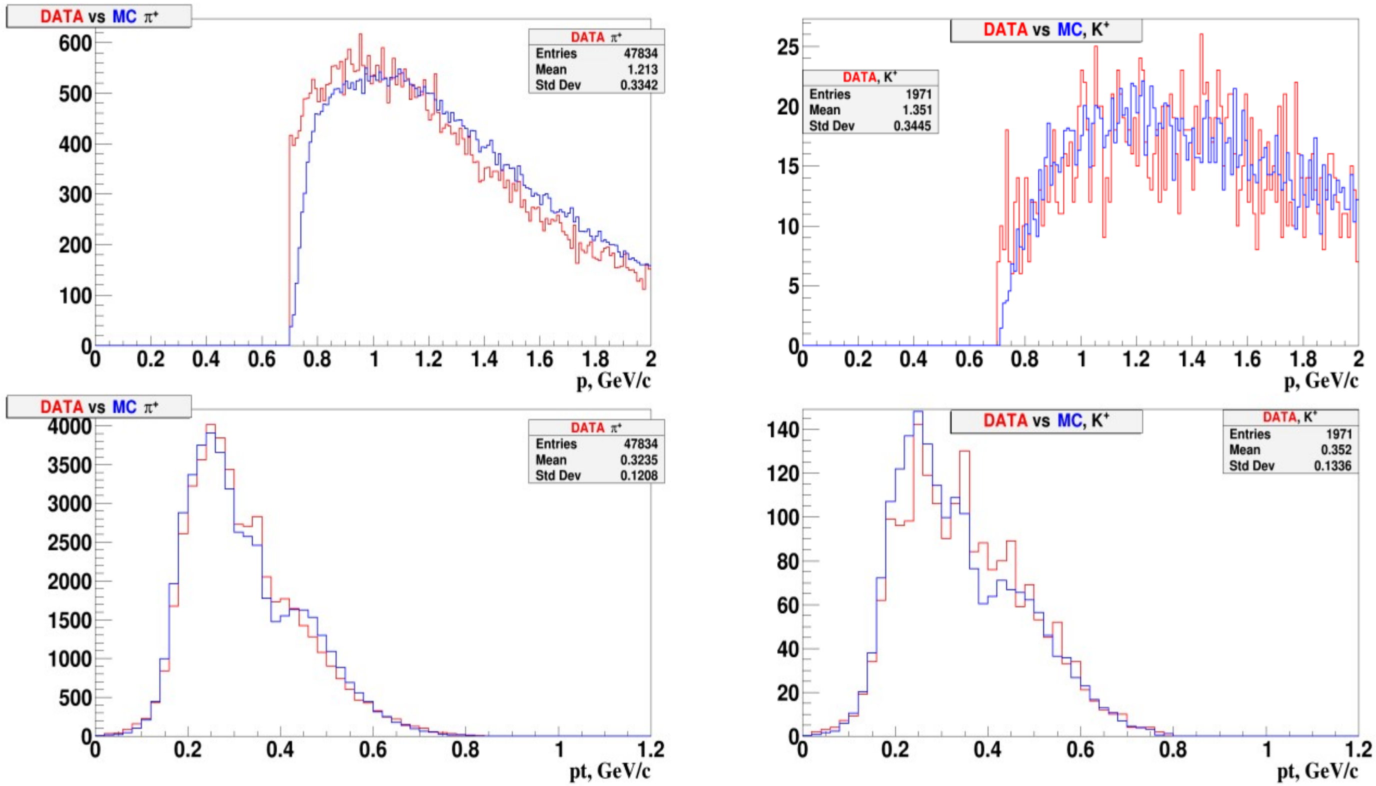

Fig. 3c. *Ar+A* interactions at 3.2 AGeV argon beam energy: comparison of *ToF-700* experimental data (red curves) and DCM-SMM + GEANT Monte Carlo simulation (blue curves): total momentum of identified π^+ and K^+ (upper plots); transverse momentum of π^+ and K^+ (lower plots).

Decomposition of efficiency

Table 4. Decomposition of π^+/K^+ reconstruction efficiency.

Reconstruction efficiency	$\varepsilon_{rec} = \varepsilon_{acc} \cdot \varepsilon_{cuts}$
π^+/K^+ geometrical acceptance in detectors	$\varepsilon_{acc} = N_{acc}\,(y,p_T) \,/\, N_{gen}\,(y,p_T)$
Efficiency of reconstruction of π^+/K^+ within the detector geometrical acceptance after applying kinematic and spatial cuts	$\varepsilon_{cuts} = N_{rec}(y,p_T) \,/\, N_{acc}(y,p_T)$

After the event simulation and reconstruction the successfully reconstructed π^+/K^+ were counted in the numerator N_{acc}. The detector acceptance was taken as N_{acc}/N_{gen}, where N_{gen} is the total number of generated MC events. The number of π^+/K^+ after applying kinematic and spatial cuts (N_{cuts}) gave the "selection cuts" efficiency with respect to the number of accepted ones from above.

Efficiency in *Ar+Cu* interactions for π^+

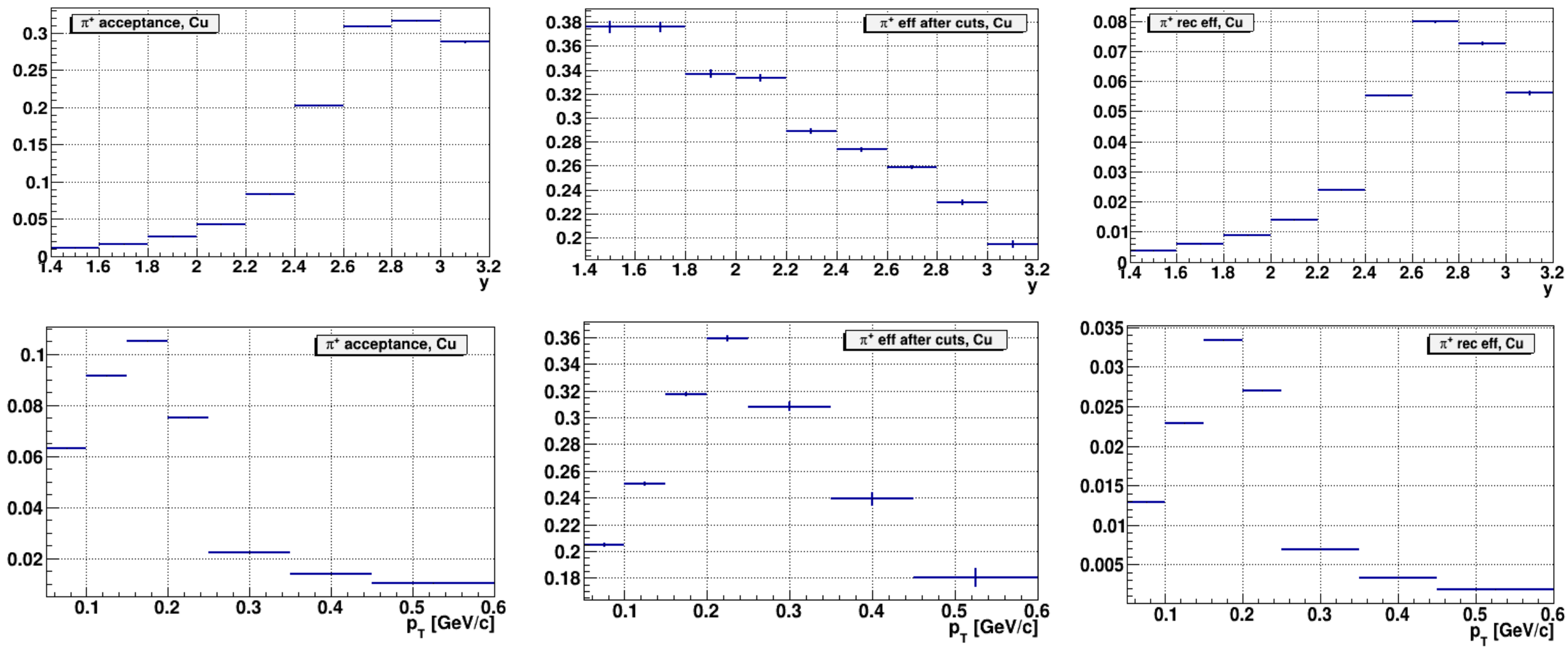

Fig.12a. π^+ geometrical acceptance (left plots); efficiency of reconstruction of accepted π^+ after applying kinematic and spatial cuts (middle plots) and full reconstruction efficiency (right plots) shown in bins of rapidity y lab in the laboratory system, transverse momentum p_T.

Results are shown for *Ar+Cu* interactions at 3.2 AGeV argon beam energy.

Efficiency in *Ar+Cu* interactions for K^+

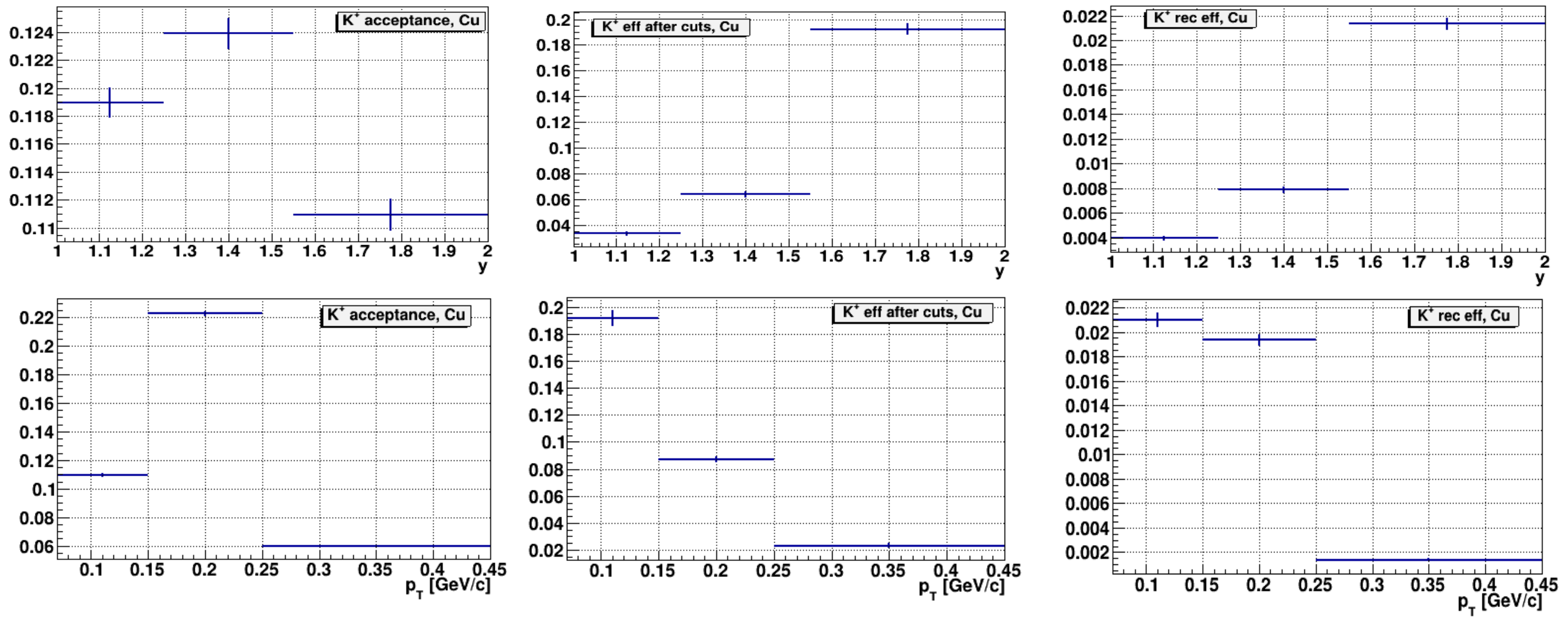

Fig.12b. K^+ geometrical acceptance (left plots); efficiency of reconstruction of accepted K^+ after applying kinematic and spatial cuts (middle plots) and full reconstruction efficiency (right plots) shown in bins of rapidity y lab in the laboratory system, transverse momentum p_T.
Results are shown for *Ar+Cu* interactions at 3.2 AGeV argon beam energy.

Trigger efficiency for Barrel Detector

Table 5a. Mean BD trigger efficiency evaluated for events with reconstructed π^+/K^+ in interactions of the argon beam with the whole set of *C*, *Al*, *Cu*, *Sn*, *Pb* targets.

Trigger / Target **π^+ mesons**	***C***	***Al***	***Cu***	***Sn***	***Pb***
ε_{trig} (BD>=2)	0.80±0.03	0.96±0.01	0.98±0.01	0.99±0.01	0.99±0.01
ε_{trig} (BD>=3)	0.66±0.02	0.92±0.01	0.97±0.01	0.98±0.01	0.99±0.01
ε_{trig} (BD>=4)	0.48±0.02	0.88±0.01	0.95±0.01	0.97±0.01	0.98±0.01

Trigger / Target **K^+ mesons**	***C***	***Al***	***Cu***	***Sn***	***Pb***
ε_{trig} (BD>=2)	0.67±0.15	0.97±0.02	0.98±0.01	0.99±0.01	0.99±0.01
ε_{trig} (BD>=3)	0.67±0.15	0.96±0.02	0.97±0.01	0.99±0.01	0.99±0.01
ε_{trig} (BD>=4)	0.67±0.15	0.94±0.02	0.95±0.02	0.99±0.01	0.98±0.01

Trigger efficiency for Forward Silicon

Table 5b. Mean FD trigger efficiency evaluated for events with reconstructed π^+/K^+ in interactions of the argon beam with the whole set of *C*, *Al*, *Cu*, *Sn*, *Pb* targets.

Trigger / Target π^+ mesons	***C***	***Al***	***Cu***	***Sn***	***Pb***
ε_{trig} (FD>=2)	0.28±0.01	0.40±0.01	0.56±0.01	0.65±0.01	0.72±0.01
ε_{trig} (FD>=3)	0.14±0.01	0.22±0.01	0.37±0.01	0.49±0.01	0.58±0.01
ε_{trig} (FD>=4)	0.08±0.01	0.11±0.01	0.23±0.01	0.34±0.01	0.46±0.01

Trigger / Target K^+ mesons	***C***	***Al***	***Cu***	***Sn***	***Pb***
ε_{trig} (FD>=2)	0.30±0.06	0.40±0.03	0.64±0.03	0.74±0.03	0.82±0.03
ε_{trig} (FD>=3)	0.17±0.04	0.23±0.02	0.45±0.03	0.61±0.03	0.73±0.03
ε_{trig} (FD>=4)	0.08±0.03	0.12±0.02	0.35±0.03	0.44±0.03	0.58±0.03

Luminosity

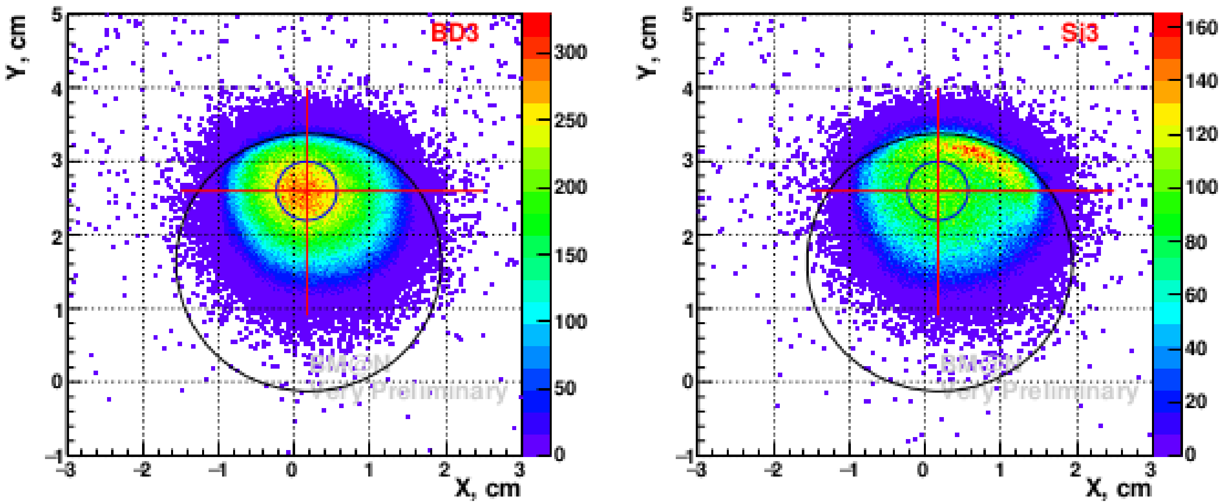

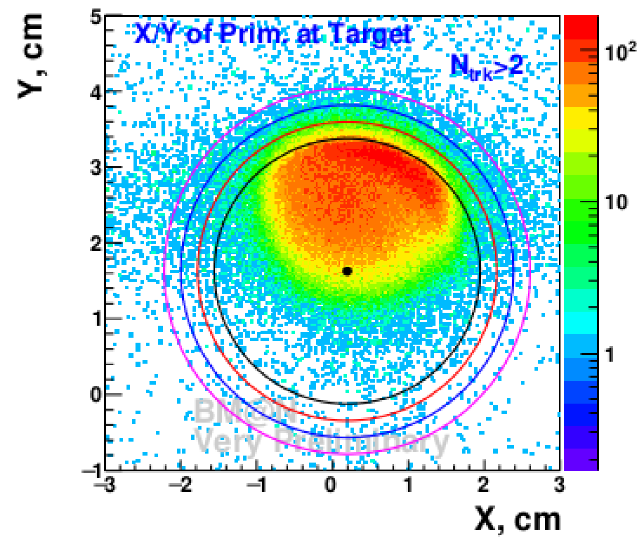

Fig.5 (lumi.pdf). Run-7, X-Y of the primary vertices for different trigger conditions. Left: *BD* ≥ 3, Right, *Si* ≥ 3.

Fig.6 (lumi.pdf). Run-7, X-Y of the primary vertices within 3−σlimits around the target.

- ✓ 13.5% of the beam is missed the target by the edge of the target due to shifted beam position.
- ✓ The systematic uncertainty for this measurement do not exceed 2%.
- ✓ The events collected with the Si-trigger near the upper edge of the target were recorded with higher efficiency relative the rest of the beam spot.

Impact parameters

Table 1*. Mean impact parameters of min. bias *Ar+C*, *Ar+Al*, *Ar+Cu*, *Ar+Sn*, *Ar+Pb* interactions with π^+.

MC	*b*, fm (*Ar+C*)	*b*, fm (*Ar+Al*)	*b*, fm (*Ar+Cu*)	*b*, fm (*Ar+Sn*)	*b*, fm (*Ar+Pb*)
Events with gen. π^+	4.18	4.79	5.59	6.29	7.04
Events with gen. π^+ in the measured range of BM@N	3.75	4.29	5.03	5.70	6.43
Events with rec. π^+	3.51	3.91	4.61	5.29	6.13

Table 2*. Mean impact parameters of min. bias *Ar+C*, *Ar+Al*, *Ar+Cu*, *Ar+Sn*, *Ar+Pb* interactions with K^+.

MC	*b*, fm (*Ar+C*)	*b*, fm (*Ar+Al*)	*b*, fm (*Ar+Cu*)	*b*, fm (*Ar+Sn*)	*b*, fm (*Ar+Pb*)
Events with gen. K^+	3.24	3.50	3.98	4.50	5.12
Events with gen. K^+ in the measured range of BM@N	3.17	3.42	3.90	4.44	5.13
Events with rec. K^+	3.25	3.55	4.13	4.72	5.46

Cross section and yields of π^+/K^+ mesons

The cross section $\sigma_{\pi+}$ and yield $Y_{\pi+}$ of π^+ meson production in *Ar+C*, *Ar+Al*, *Ar+Cu*, *Ar+Sn*, *Ar+Pb* interactions are calculated in bins of y and p_T according to the formulae:

$$\sigma_{\pi+}(y,p_T) = N_{rec}^{\pi+}(y,p_T) / (\varepsilon_{rec}(y,p_T) \cdot \varepsilon_{trig} \cdot L); \qquad Y_{\pi+}(y,p_T) = \sigma_{\pi+}(y,p_T) / \sigma_{inel}$$

where L is the luminosity,

$N_{rec}^{\pi+}$ – the number of reconstructed π^+ mesons,

ε_{rec} – the combined efficiency of the π^+ meson reconstruction,

ε_{trig} – the trigger efficiency,

σ_{inel} – the cross section for minimum bias inelastic *Ar+A* interactions.

The same formulas are used to calculate the K^+ inclusive production cross section and yield in bins of $y(p_T)$. The cross sections in (y, p_T) bins are calculated as weighted averaged of the results obtained with *ToF-400* and *ToF-700* data taking into account the statistical uncertainties ($w \sim 1/\sigma^2$).

Interaction	***Ar+C***	***Ar+Al***	***Ar+Cu***	***Ar+Sn***	***Ar+Pb***
Inelastic cross section, mb	1470±50	1860±50	2480±50	3140±50	3970±50

The cross sections for inelastic *Ar+Al*, *Ar+Cu*, *Ar+Sn*, *Ar+Pb* interactions are taken from the predictions of the DCM-SMM model which are consistent with the results calculated by the formula: $\sigma_{inel} = \pi R_0^2 (A_P^{1/3} + A_T^{1/3})^2$, where $R_0 = 1.2$ fm is an effective nucleon radius, A_P and A_T are atomic numbers of the beam and target nucleus.

Number of reconstructed π^+ mesons

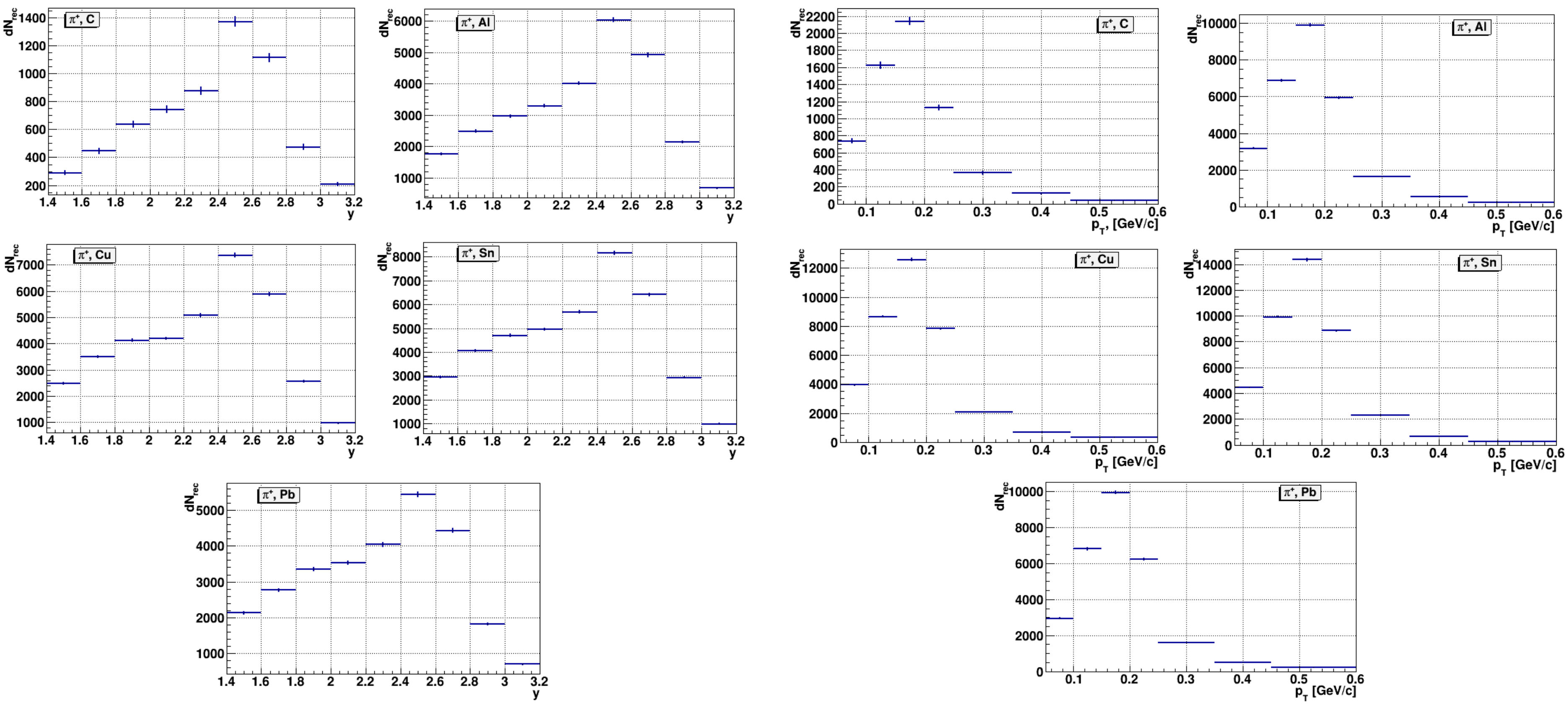

Fig. 11a. Number of reconstructed π^+ in *ToF-400* in interactions of 3.2 AGeV argon beam with *C*, *Al*, *Cu*, *Sn*, *Pb* targets in bins of y (5 left plots) and in bins of p_T (5 right plots).

Number of reconstructed K^+ mesons

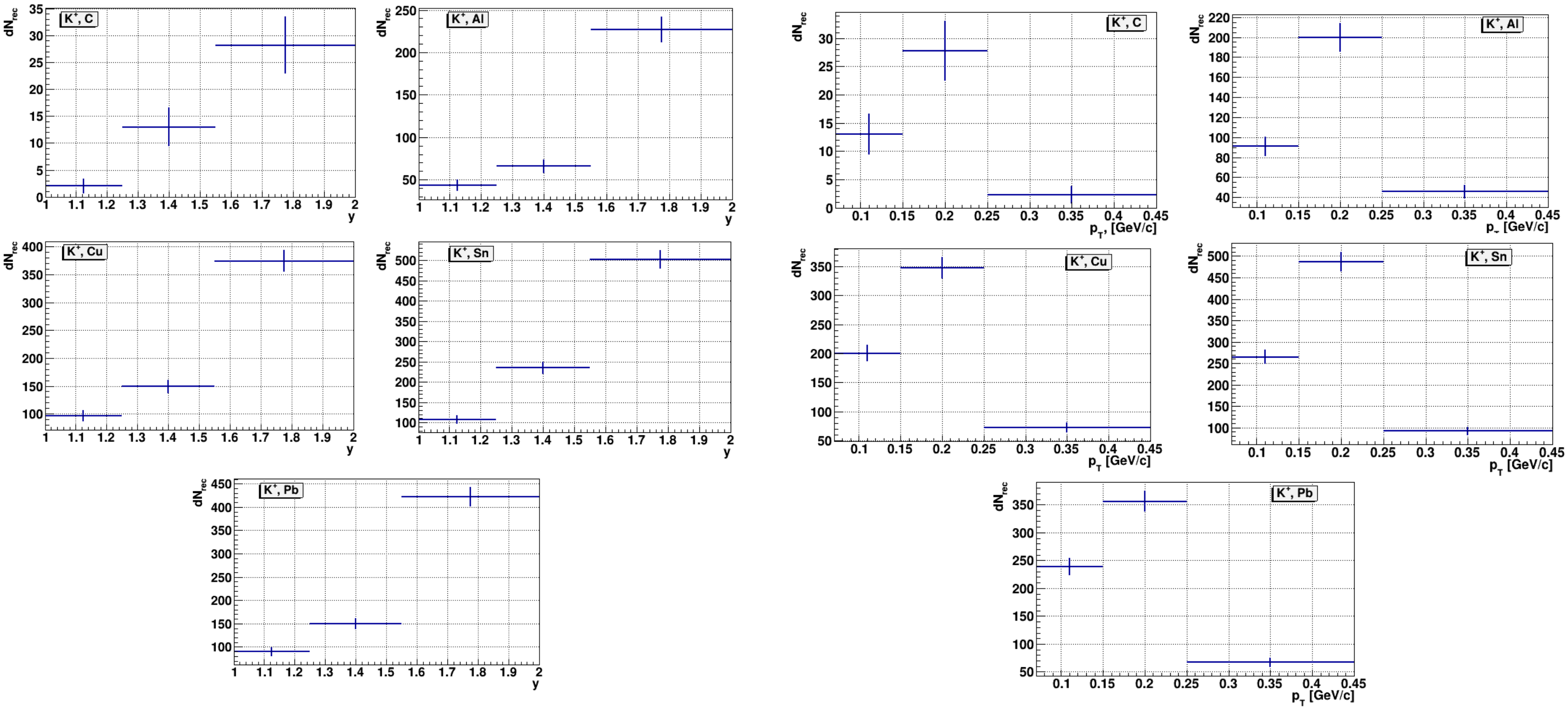

Fig. 11b. Number of reconstructed K^+ in *ToF-400* in interactions of 3.2 AGeV argon beam with *C*, *Al*, *Cu*, *Sn*, *Pb* targets in bins of y (5 left plots) and in bins of p_T (5 right plots).

Reconstructed y spectra of π^+ mesons

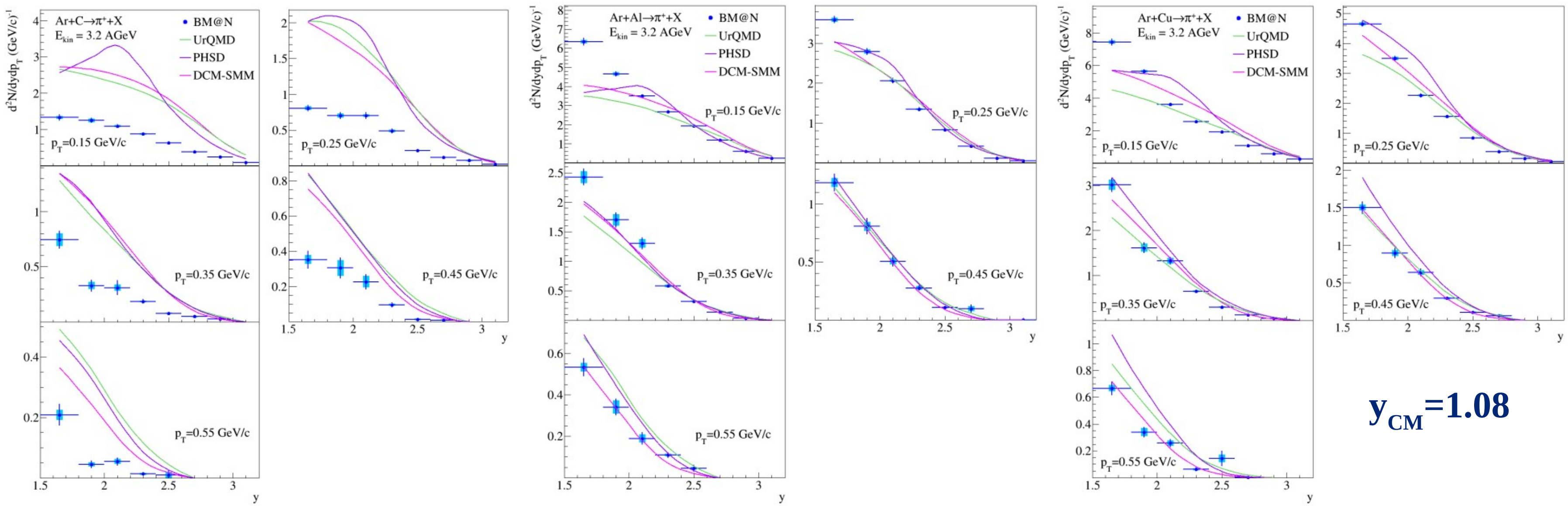

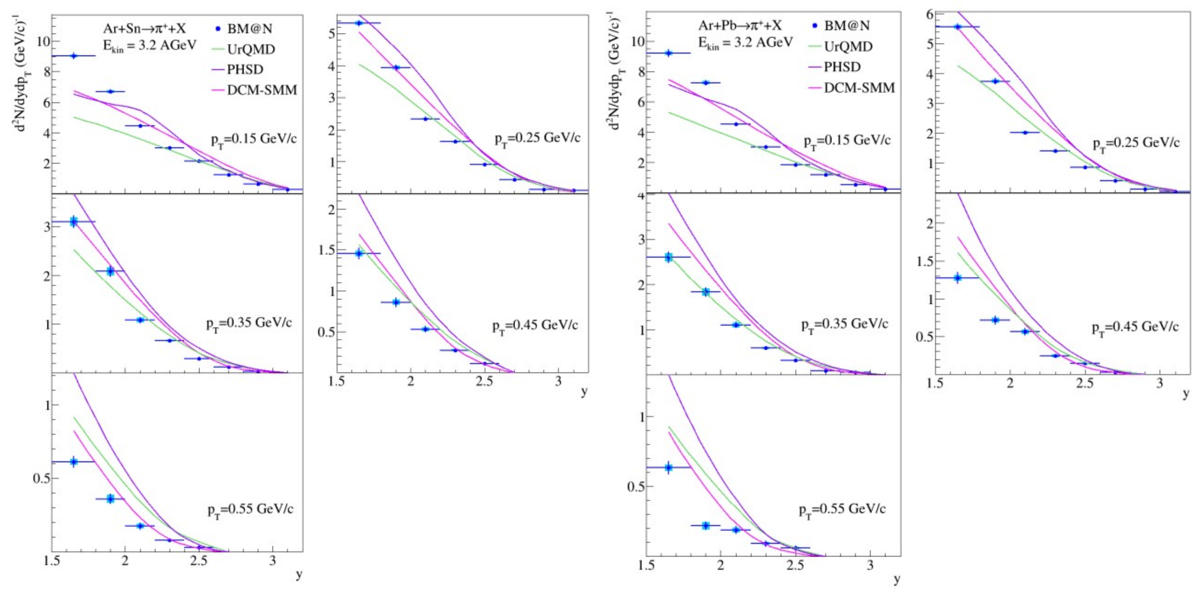

Fig. 15a. Reconstructed rapidity y spectra of π^+ measured in bins of p_T in minimum bias *Ar+C*, *Ar+Al*, *Ar+Cu*, *Ar+Sn*, *Ar+Pb* interactions at 3.2 AGeV argon beam energy (blue symbols). The error bars represent the statistical errors, the boxes show the systematic errors. Predictions of the DCM-SMM, UrQMD and PHSD models are shown as rose, green and magenta lines.

Reconstructed *y* spectra of K^+ mesons

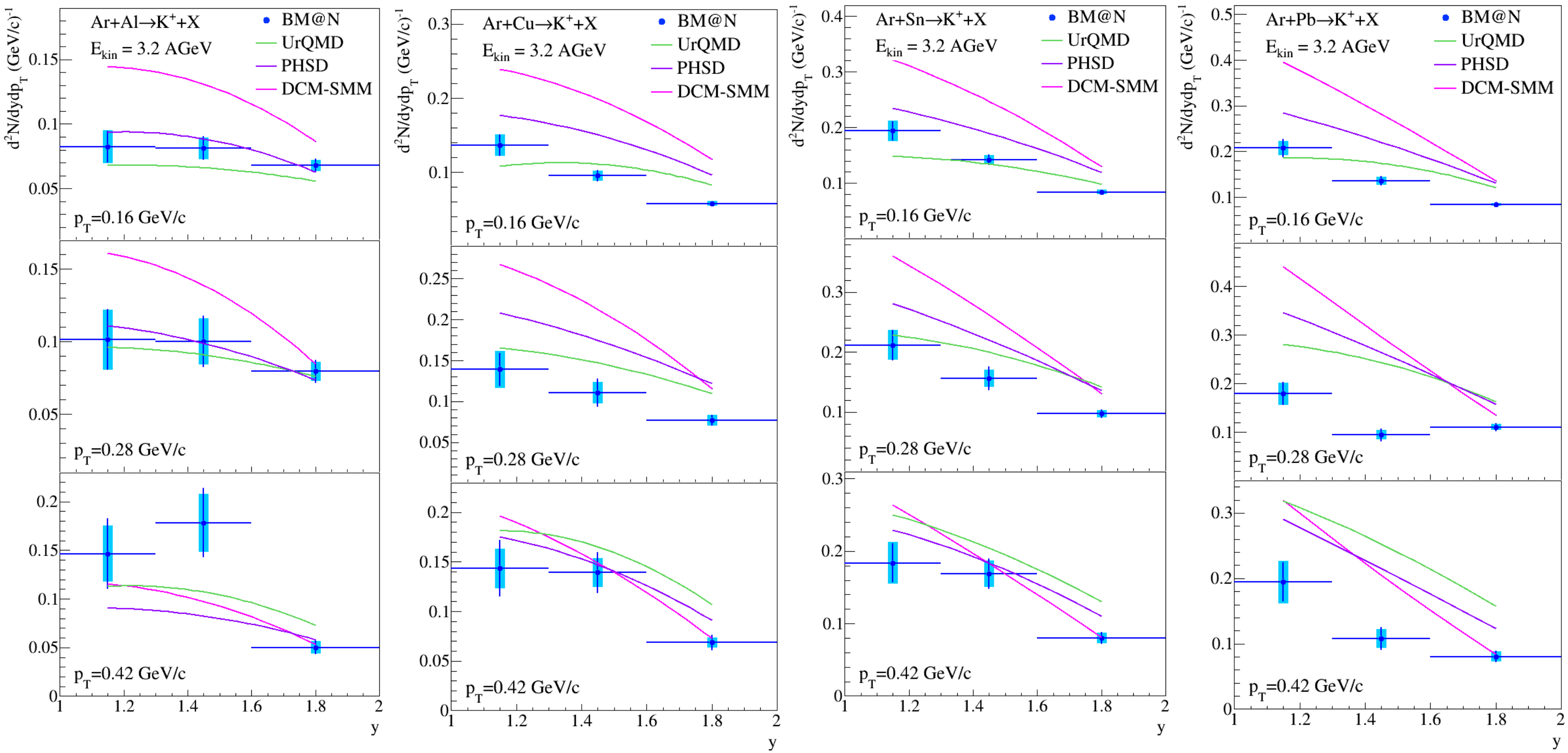

Fig. 15b. Reconstructed rapidity *y* spectra of K^+ measured in bins of p_T in minimum bias *Ar+Al*, *Ar+Cu*, *Ar+Sn*, *Ar+Pb* interactions at 3.2 AGeV argon beam energy (blue symbols). Predictions of the DCM-SMM, UrQMD and PHSD models are shown as rose, green and magenta lines.

Reconstructed p_T spectra of π^+ mesons

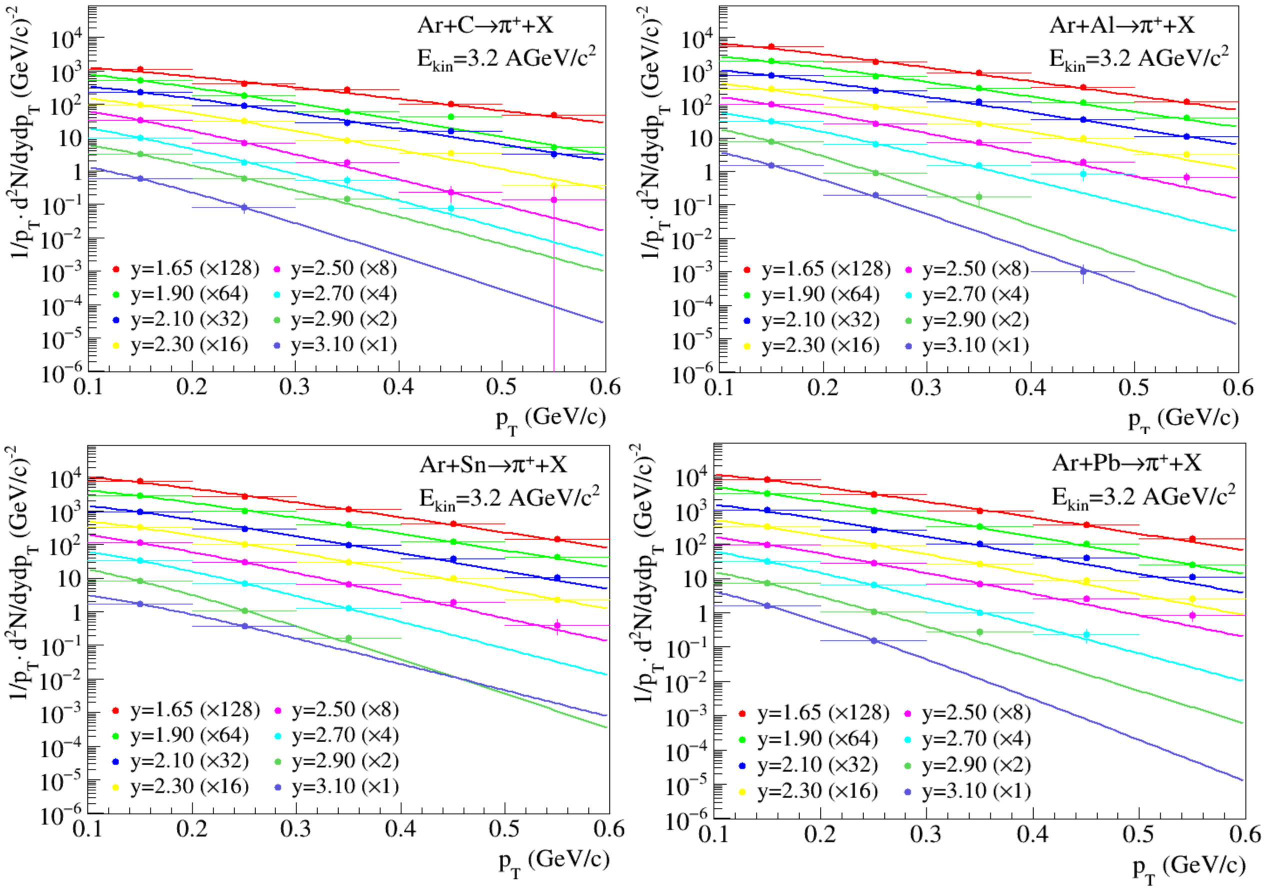

Fig. 16a. Reconstructed invariant transverse momentum p_T spectra of π^+ measured in bins of rapidity in minimum bias *Ar+C*, *Ar+Al*, *Ar+Cu*, *Ar+Sn*, *Ar+Pb* interactions at 3.2 AGeV argon beam energy (symbols). Results of the fit are shown as curves.

$$1/p_T \cdot d^2N/dp_T dy = N \cdot \exp(-(m_T - m_{\pi+})/T)$$

where $m_T=\sqrt{(m_{\pi+}^2+p_T^2)}$ is the transverse mass, N – normalization (free parameter), T – inverse slope (free parameter), dy corresponds to the measured y_{lab} range.

Reconstructed p_T spectra of K^+ mesons

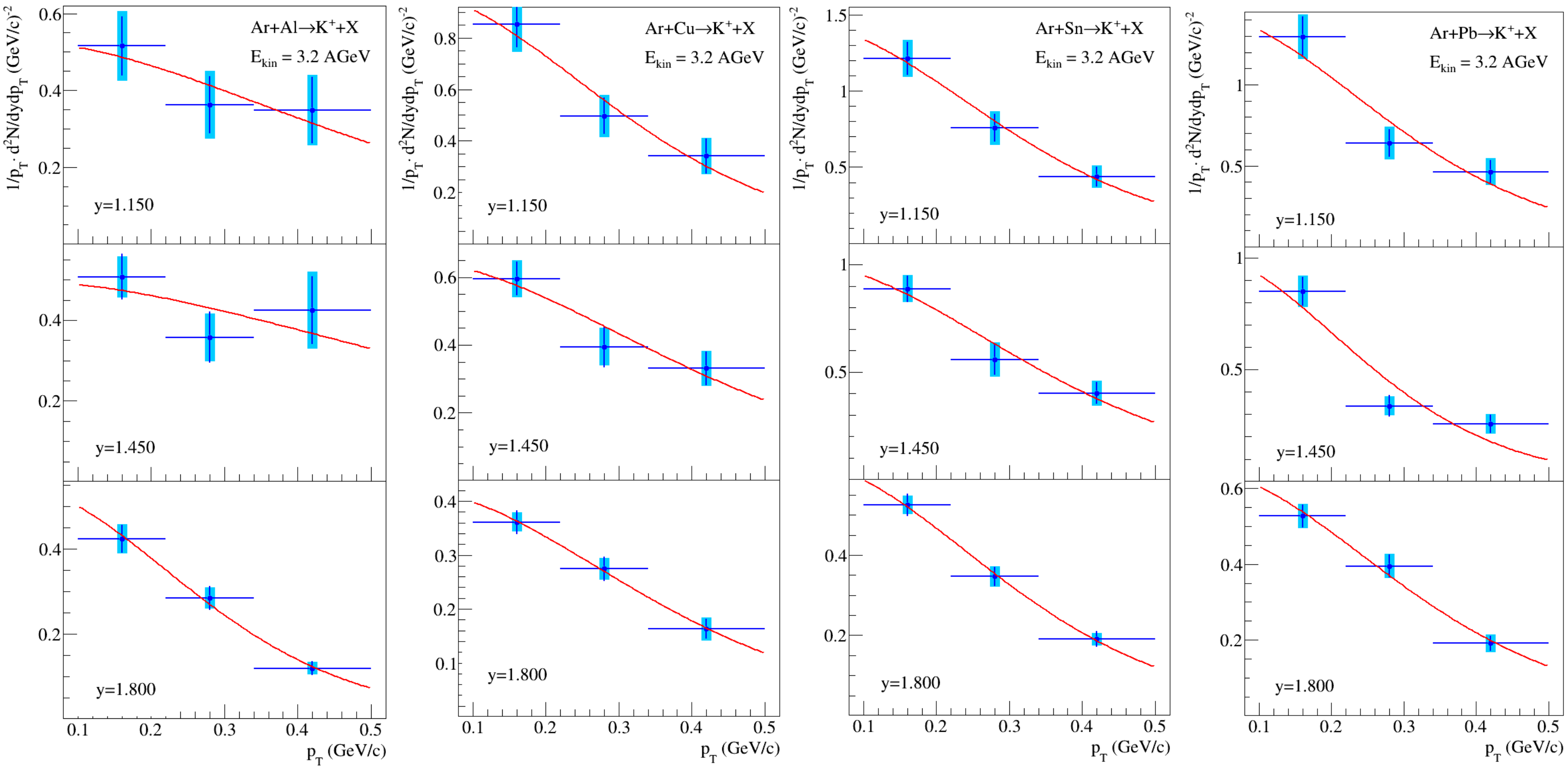

Fig. 16b. Reconstructed invariant transverse momentum p_T spectra of K^+ in minimum bias *Ar+Al*, *Ar+Cu*, *Ar+Sn*, *Ar+Pb* interactions at 3.2 AGeV argon beam energy (symbols). The error bars represent the statistical errors, the boxes show the systematic errors. Results of the fit are shown as red curves.

Reconstructed p_T spectra of K^+ mesons

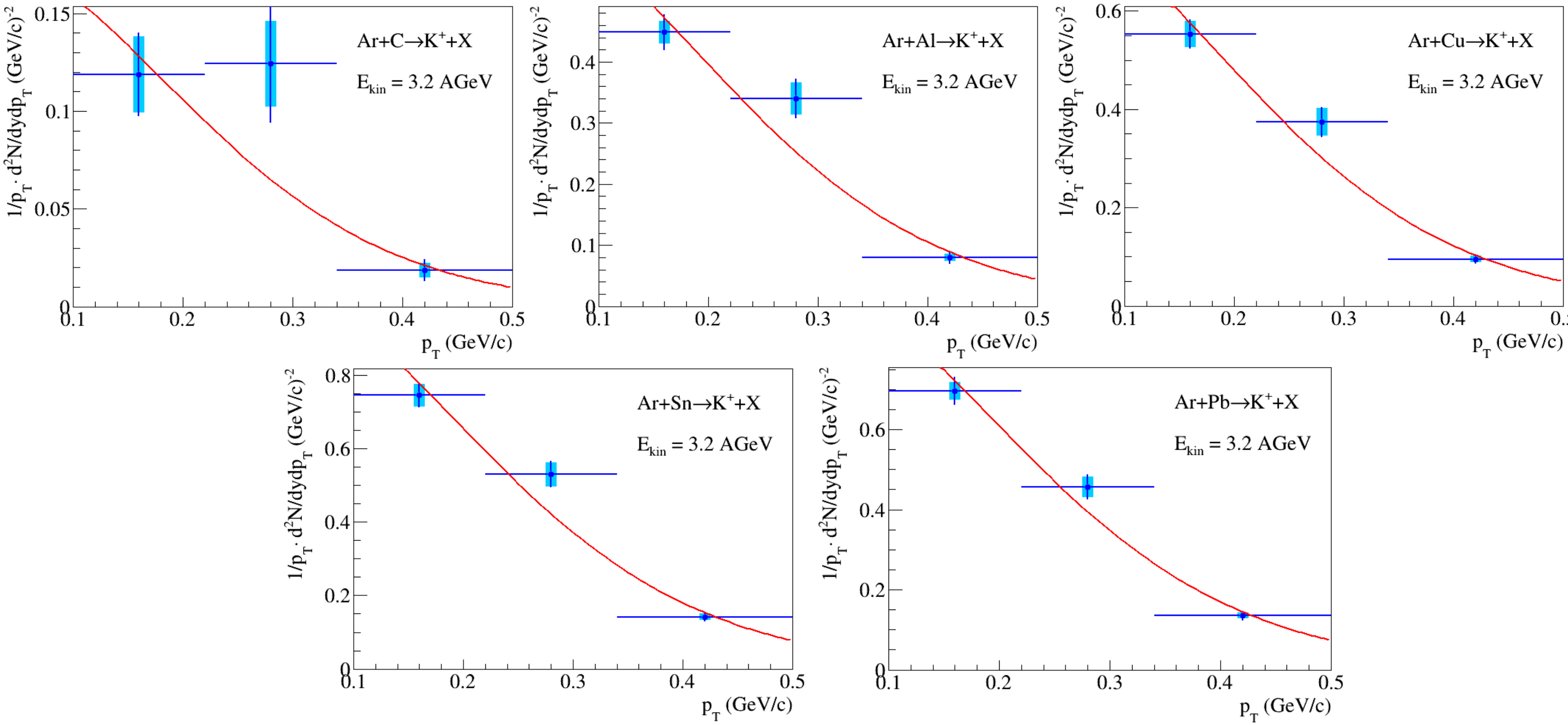

Fig. 16c. Reconstructed invariant transverse momentum p_T spectra of K^+ in the measured rapidity range in minimum bias *Ar+C*, *Ar+Al*, *Ar+Cu*, *Ar+Sn*, *Ar+Pb* interactions at 3.2 AGeV argon beam energy (symbols). Results of the fit are shown as red curves.

Inverse slope parameter T_0 of π^+ mesons

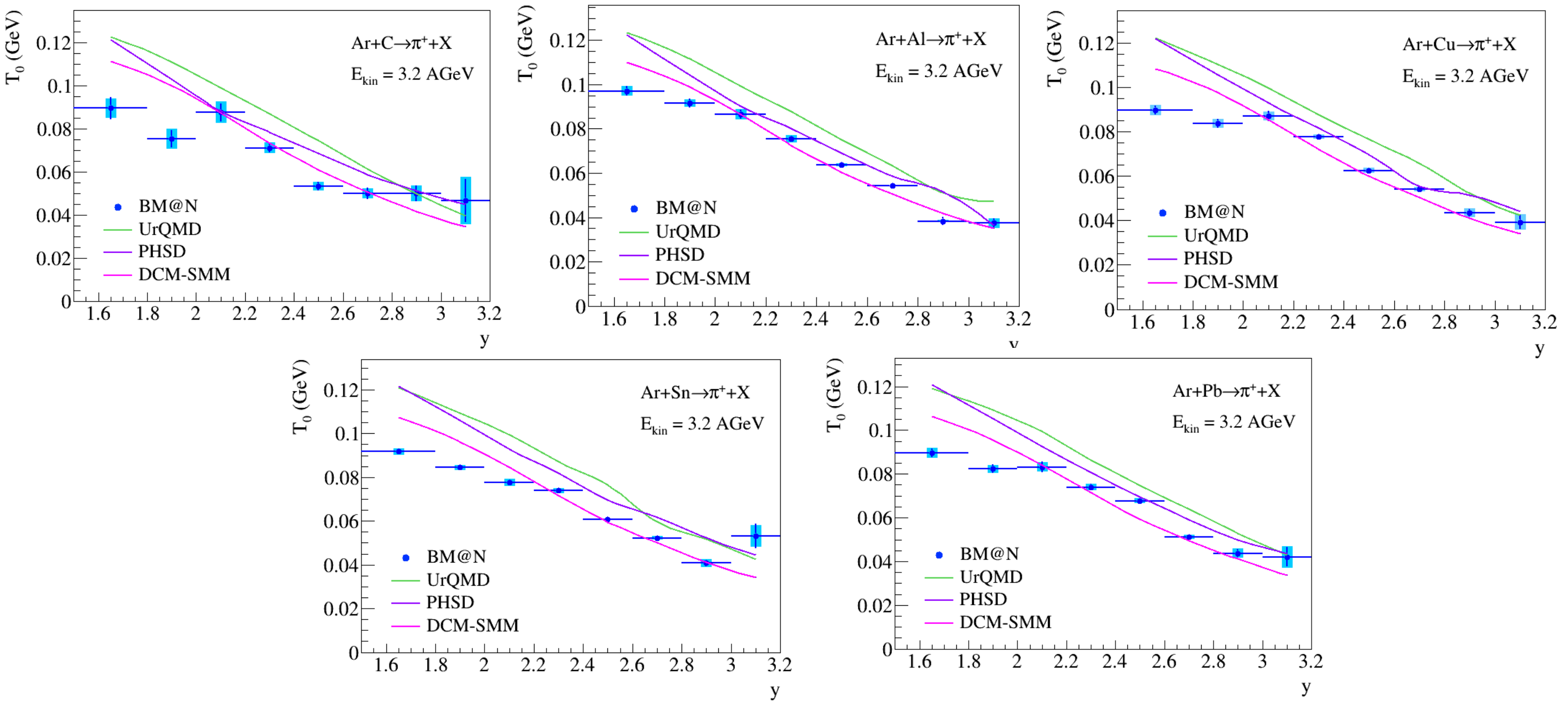

Fig. 17a. The *y* dependences of the inverse slope parameter T0 of the π^+ invariant p_T spectra in *Ar+C*, *Ar+Al*, *Ar+Cu*, *Ar+Sn*, *Ar+Pb* minimum bias interactions (blue symbols). The error bars represent the statistical errors, the boxes show the systematic errors. Predictions of the DCM-SMM, UrQMD and PHSD models are shown as rose, green and magenta lines.

Inverse slope parameter T_0 of π^+ mesons

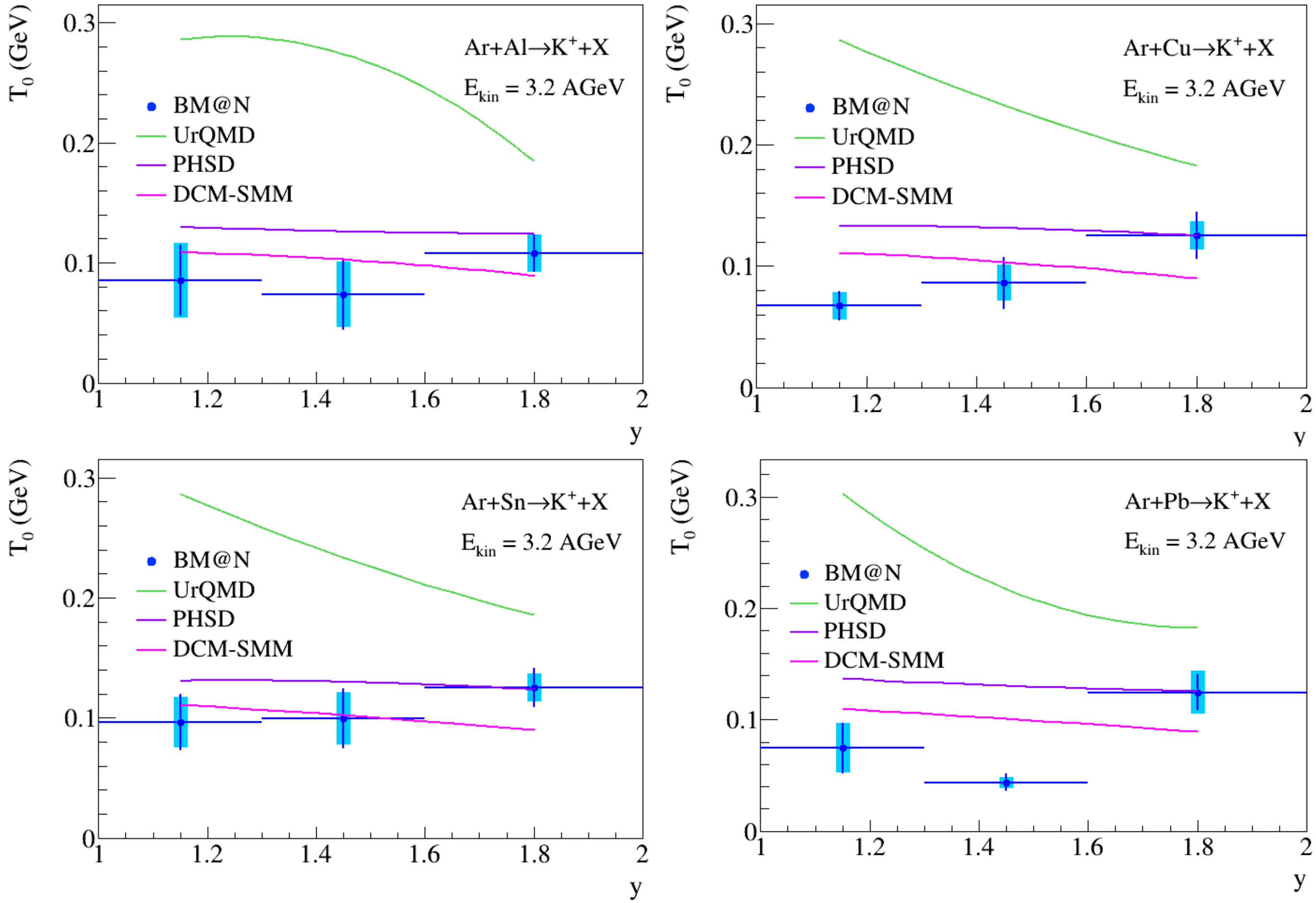

Fig. 17b. The *y* dependences of the inverse slope parameter T0 of the K^+ invariant p_T spectra in *Ar+Al*, *Ar+Cu*, *Ar+Sn*, *Ar+Pb* minimum bias interactions (blue symbols). Predictions of the DCM-SMM, UrQMD and PHSD models are shown as rose, green and magenta lines.

Systematic uncertainties

The systematic uncertainty of the π^+/K^+ yields in every p_T and y bin is calculated as a quadratic sum of uncertainties coming from the following sources:

Sys1: Systematic uncertainty of the trigger efficiency evaluated as a function of the number of tracks from the primary vertex and the primary vertex position.

Sys2: Systematic uncertainties of the reconstruction efficiency due to the remaining difference in the X/Y primary vertex distribution in the simulation relative to the experimental data.

Sys3: Systematic uncertainties of the background subtraction under the π^+ and K^+ signals in the mass squared spectra of identified particles.

Table 10. Total systematic uncertainty of the π^+ and K^+ yields measured argon-nucleus interactions.

Target / Systematics	π^+					Target / Systematics	K^+				
	C, sys%	***Al***, sys%	***Cu***, sys%	***Al***, sys%	***Al***, sys%		***C***, sys%	***Al***, sys%	***Cu***, sys%	***Sn***, sys%	***Pb***, sys%
Sys1-Sys3	14	11	12	9	9	Sys1-Sys3	28	26	14	12	16
Norm	7.8	6.3	6.2	6.2	6.2	Norm	29	10	8.4	7.6	7.4

The π^+/K^+ yield normalization uncertainty calculated as a quadratic sum of uncertainties of the trigger efficiency, luminosity and inelastic nucleus-nucleus cross section. The normalization uncertainty is valid for the whole measured kinematical range.

The π^+ yields (BM@N)

Table 12a. Extrapolation factors to the full kinematic range and π^+ yields for 3.2 AGeV argon-nucleus data in the measured and full kinematical ranges. The first errors given are statistical, the second errors are systematic.

3.2 AGeV, π^+	*C*	*Al*	*Cu*	*Sn*	*Pb*
DCM-SMM extrap. factor	3.43	3.86	4.51	4.98	5.64
Yield in $0.1<p_T<0.6$ GeV/c, $1.5<y_{lab}<3.2$	0.275±0.006 ±0.027	1.00±0.01 ±0.07	1.14±0.01 ±0.08	1.28±0.01 ±0.09	1.25±0.01 ±0.085
Yield in the full kin. range	0.943±0.019 ±0.092	3.86±0.04 ±0.27	5.15±0.05 ±0.35	6.35±0.05 ±0.44	7.03±0.07 ±0.48

The K^+ yields (BM@N)

Table 12b. Extrapolation factors to the full kinematic range, K^+ yields and K^+ to π^+ yield ratios for 3.2 AGeV data in the measured and full kinematical ranges. The first errors given are statistical, the second errors are systematic. Also the inverse slope parameters T of the invariant p_T spectra are given.

3.2 AGeV, K^+	***C***	***Al***	***Cu***	***Sn***	***Pb***
DCM-SMM extrap. factor	2.33	2.51	2.84	3.21	3.67
Yield in $0.1<p_T<0.5$ GeV/c, $1.0<y_{lab}<2.0$	0.0094±0.0018 ±0.0035	0.0390±0.0028 ±0.0061	0.0417±0.0021 ±0.0066	0.0560±0.0022 ±0.0075	0.0510±0.0022 ±0.0092
Yield in the full kin. range	0.0219±0.0042 ±0.0081	0.0980±0.0070 ±0.015	0.1190±0.0060 ±0.019	0.180±0.007 ±0.024	0.188±0.008 ±0.034
K^+/π^+ ratio in the measured range	0.0343±0.0066 ±0.0125	0.0390±0.0028 ±0.0055	0.0366±0.0019 ±0.0053	0.0439±0.0018 ±0.0051	0.0411±0.0018 ±0.0068
K^+/π^+ ratio in the full kin. range	0.0233±0.0045 ±0.0085	0.0253±0.0018 ±0.0035	0.0230±0.0012 ±0.0033	0.0283±0.0012 ±0.033	0.0268±0.0012 ±0.0044
K+ inverse slope T, MeV measured range	73±14±13	80±7±5	81±5±5	81±5±4	78±5±4

The π^+ and K^+ yields and inverse slopes

Table 13. Yields of K^+, π^+ production and effective inverse slopes of invariant m_T spectra measured in interactions of light and medium nucleus.

Interacting nucleus / Beam kinetic energy / Experiment	π^+, K^+ yields	K^+ / π^+ yield ratio, $\cdot 10^{-2}$	T_{eff} at $y^* = 0$, MeV, K^+ / π^+
Ar+KCl, 1.76 AGeV, HADES	$3.9\pm0.1\pm0.1$ (π^-) $(2.8\pm0.2)\cdot10^{-2}$ (K^+)		$82.4\pm0.1^{+9.1}_{-4.6}$ (π^-) $89\pm1\pm2$ (K^+)
Ni+Ni, 1.93 AGeV, FOPI	$3.6\cdot10^{-2}$ (K^+, $A_{part} = 46.5$) $8.25\cdot10^{-2}$(K^+, $A_{part} = 75$)	$(7.59\pm0.49)\cdot10^{-3}$ ($A_{part} = 46.5$)	110.9 ± 1.0 ($A_{part} = 75$)
Ni+Ni, 1.93 AGeV, KaoS	$3\cdot10^{-2}$ (K^+)		97 ± 7 (non-central) (K^+) 107 ± 10 (central)(K^+)

Summary

1. Production of π^+ and K^+ mesons in interactions of the 3.2A GeV kinetic energy argon beam with *C*, *Al*, *Cu*, *Sn*, *Pb* targets was studied with the BM@N detector at the Nuclotron.
2. The analysis procedure has been presented and described.
3. Results on π^+ and K^+ meson yields and inverse slope parameters have been obtained and compared with model predictions and data available.
4. Draft article released 21.08.2022. Waiting for comments. Deadline 30 September 23:59.
5. Request for publication.

Thank you for attention!

Backup

Efficiency distributions in Si/GEMs

Si-2 GEM-3

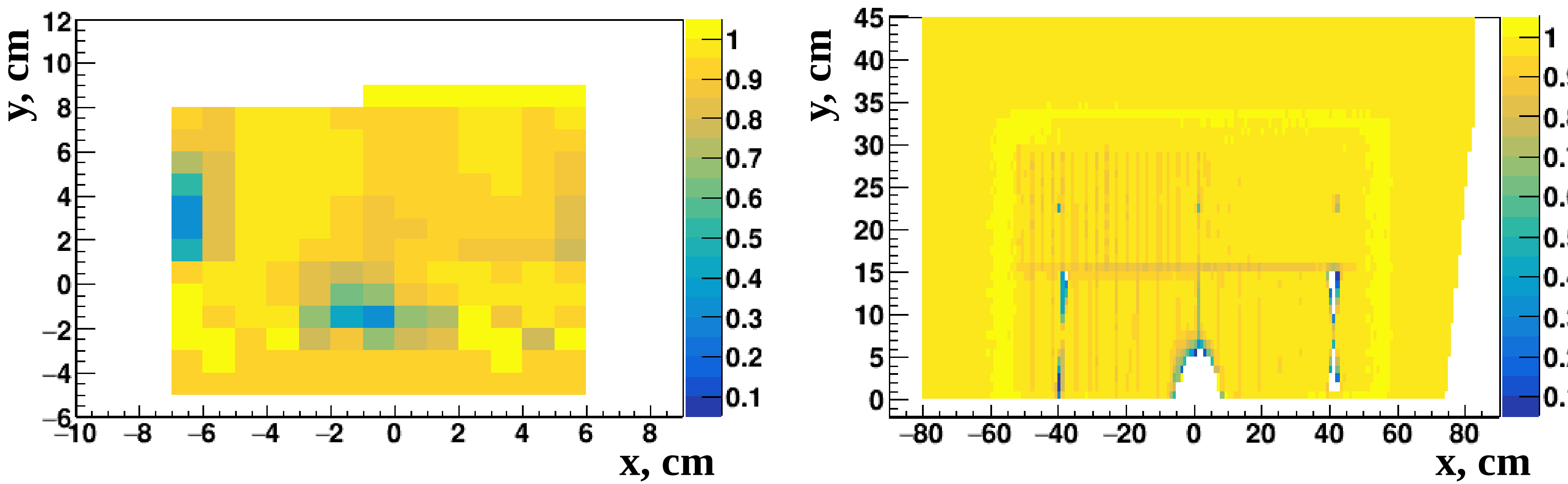

Fig. 4. 2-dimentional efficiency distributions in Si and GEM stations measured with experimental tracks and implemented into Monte Carlo simulation

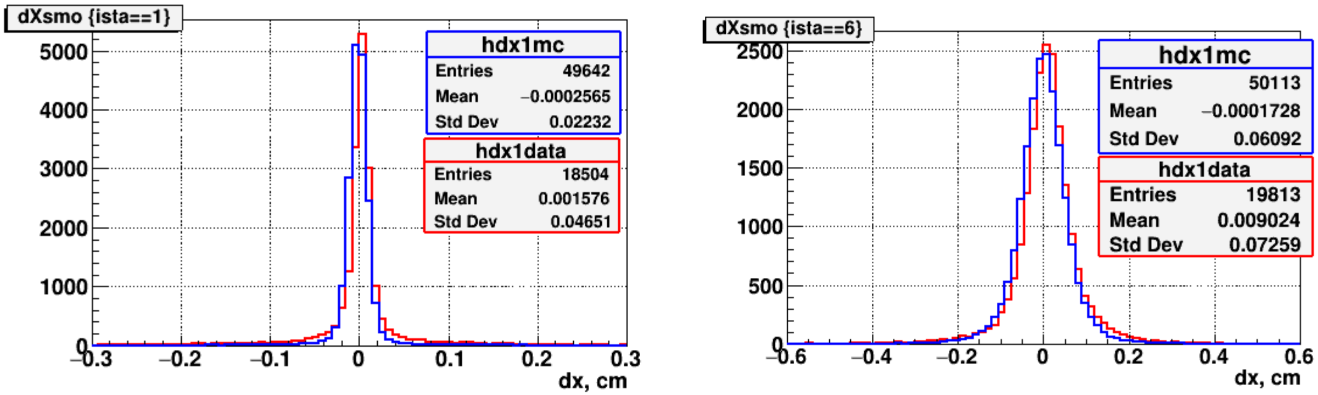

Fig. 5a. Residual distributions of hits in X projection with respect to reconstructed tracks in *Si* and *GEM* detectors: experimental data (red histograms), simulated tracks (blue histograms).

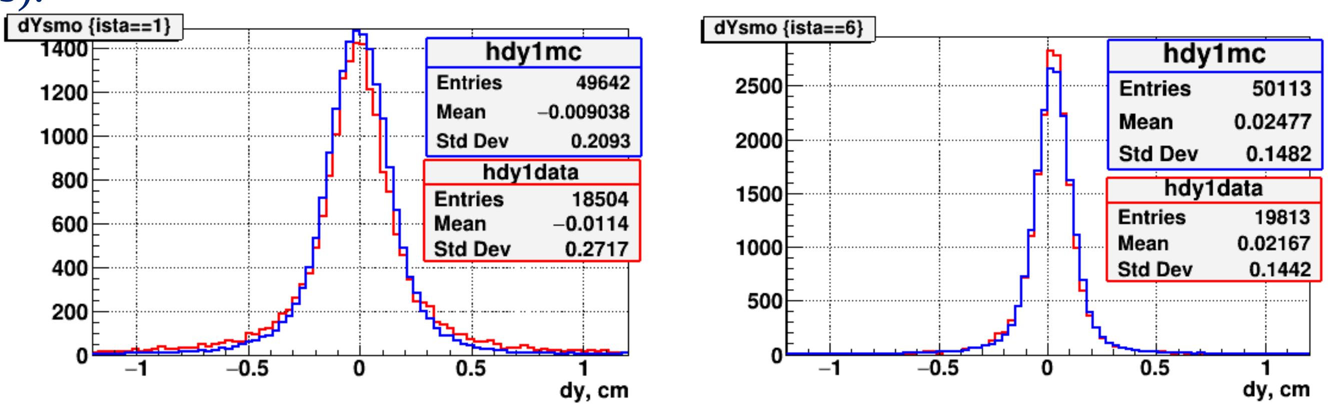

Fig. 5b. Residual distributions of hits in Y projection with respect to reconstructed tracks in *Si* and *GEM* detectors: experimental data (red histograms), simulated tracks (blue histograms).

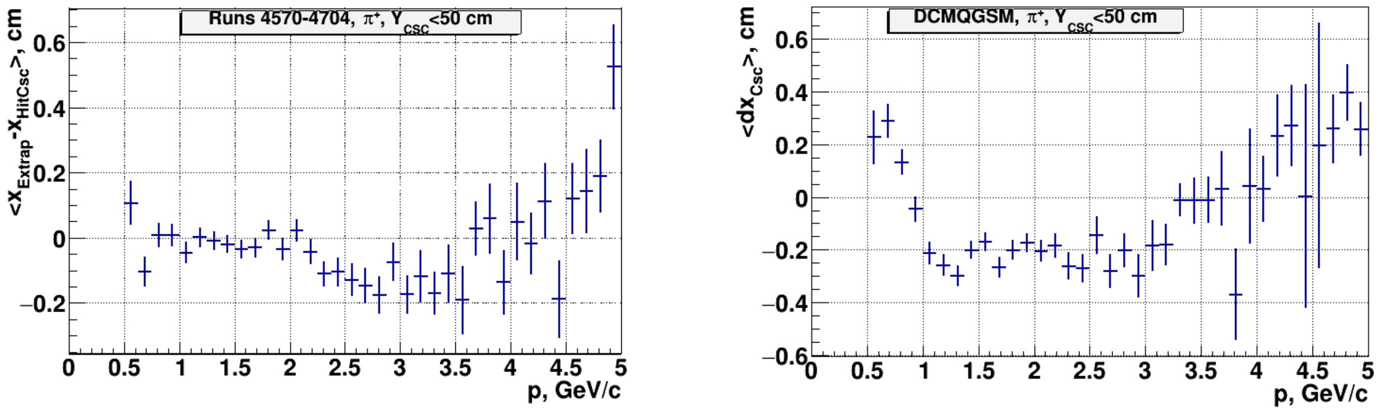

Fig. 6a. *ToF-400* data and simulation: Mean values of residuals of *CSC* hits in X projection with respect to reconstructed positive tracks in dependence on the particle momentum: left plot – experimental data, right plot – simulated tracks.

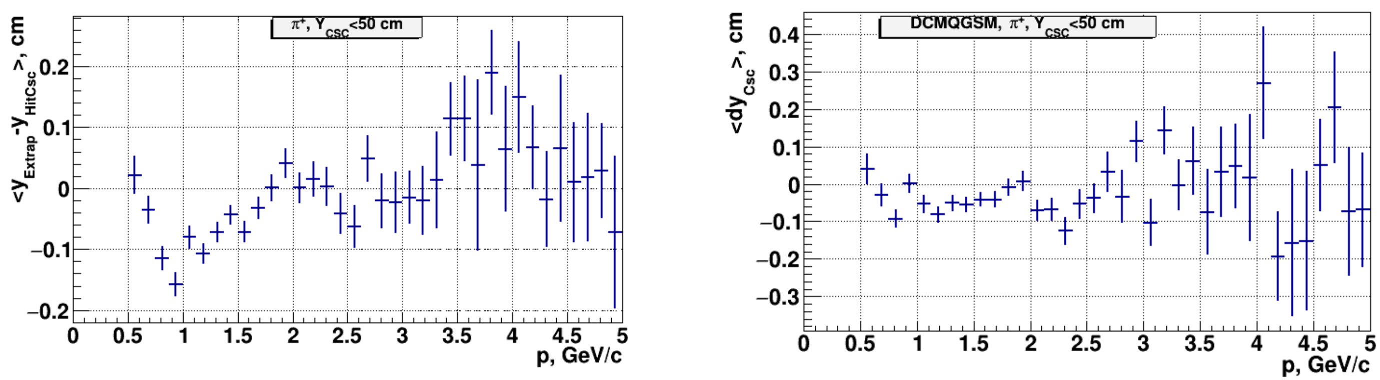

Fig. 6b. *ToF-400* data and simulation: Mean values of residuals of *CSC* hits in Y projection with respect to reconstructed positive tracks in dependence on the particle momentum: left plot – experimental data, right plot – simulated tracks.

Sigma of residuals of *CSC* hits

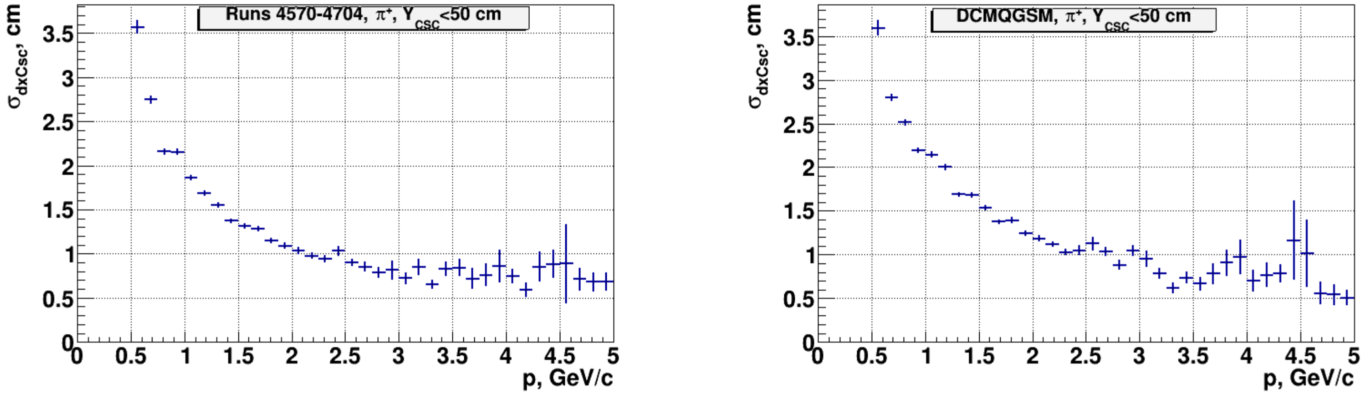

Fig. 6c. *ToF-400* data and simulation: Sigma of residuals of *CSC* hits in X projection with respect to reconstructed positive tracks in dependence on the particle momentum: left plot – experimental data, right plot – simulated tracks.

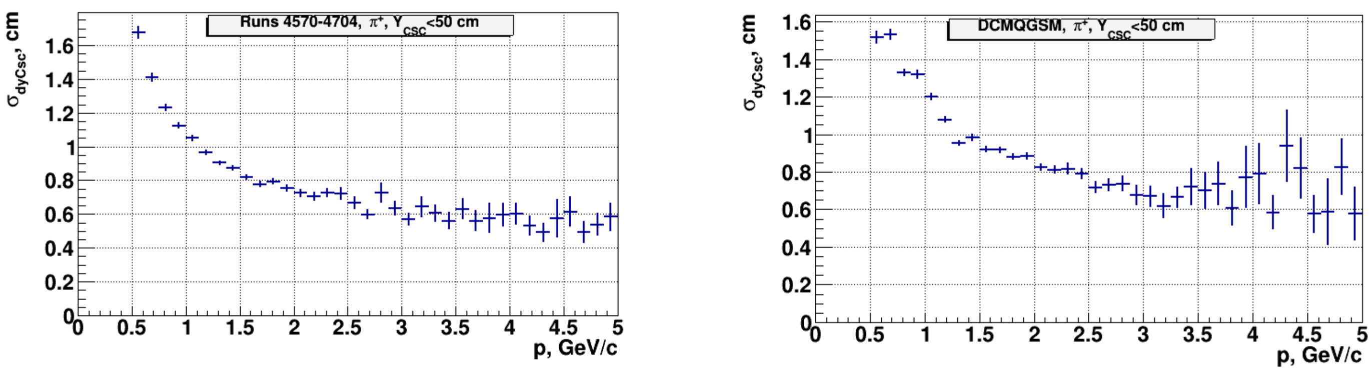

Fig. 6d. *ToF-400* data and simulation: Sigma of residuals of *CSC* hits in Y projection with respect to reconstructed positive tracks in dependence on the particle momentum: left plot experimental data, right plot – simulated tracks.

Mean values of residuals of *ToF-400* hits

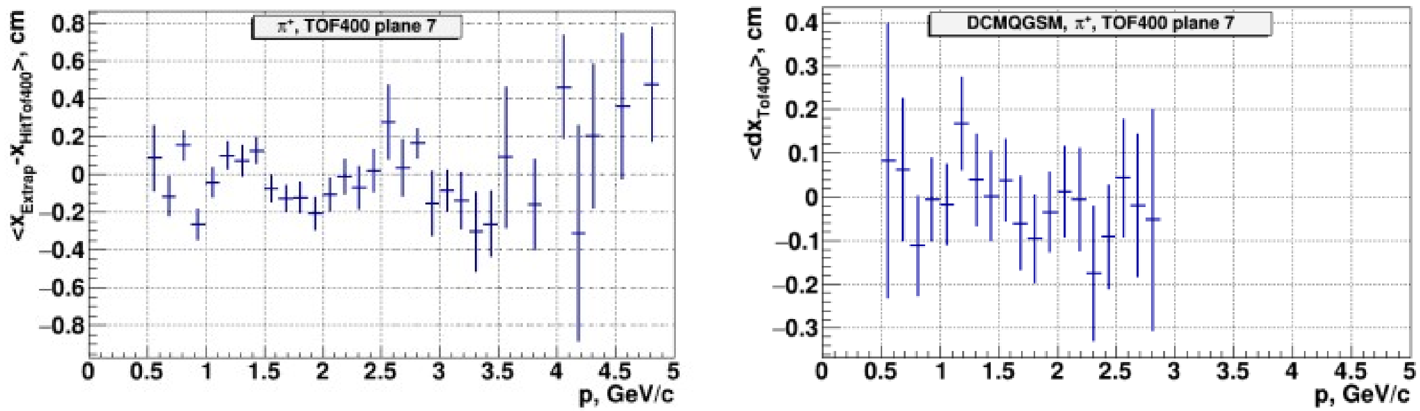

Fig. 7a. Mean values of residuals of *ToF-400* hits in the X projection with respect to reconstructed positive tracks in dependence on the particle momentum: left plot – experimental data, right plot – simulated tracks.

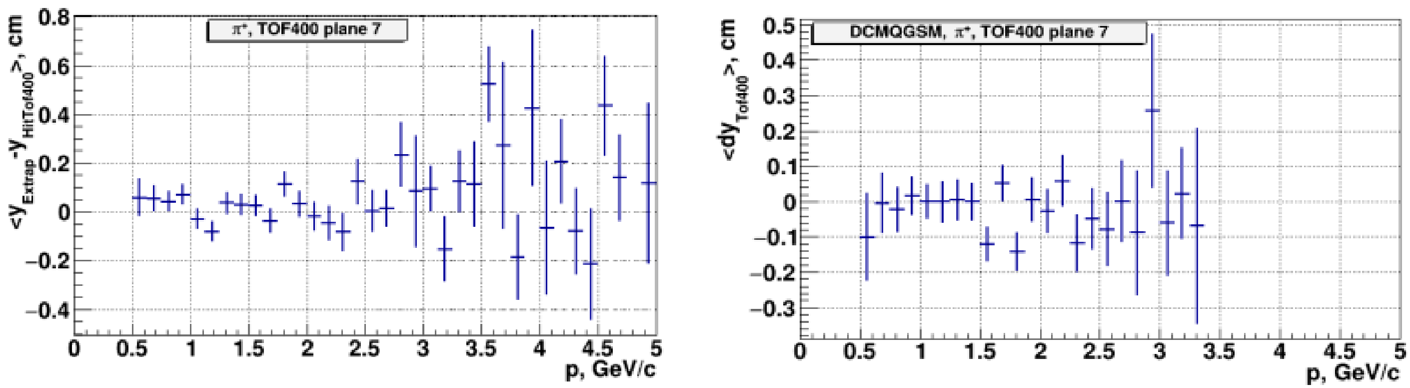

Fig. 7b. Mean values of residuals of *ToF-400* hits in the Y projection with respect to reconstructed positive tracks in dependence on the particle momentum: left plot – experimental data, right plot – simulated tracks.

Sigma of residuals of *ToF-400* hits

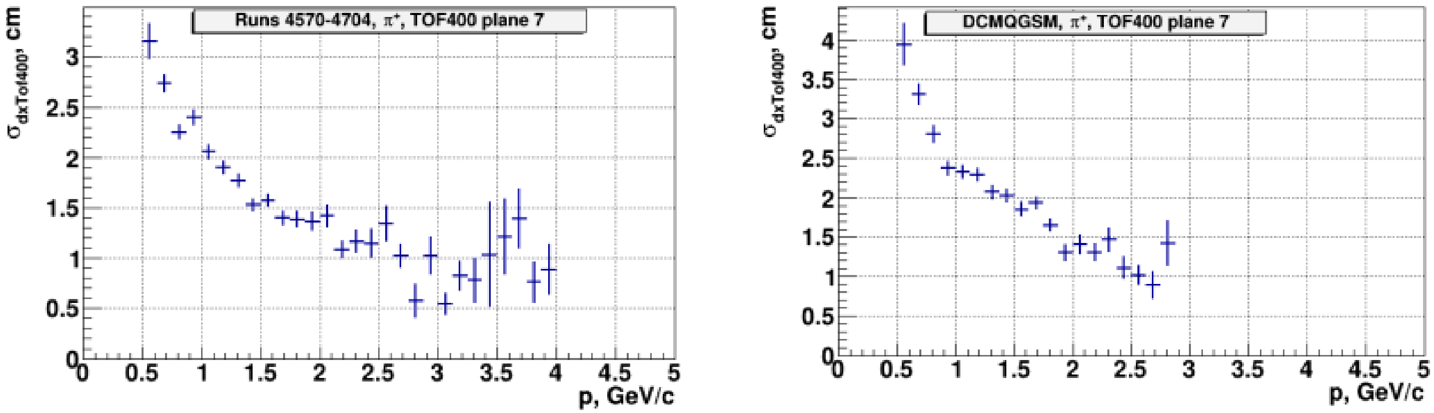

Fig. 7c. Sigma of residuals of *ToF-400* hits in the X projection with respect to reconstructed positive tracks in dependence on the particle momentum: left plot – experimental data, right plot – simulated tracks.

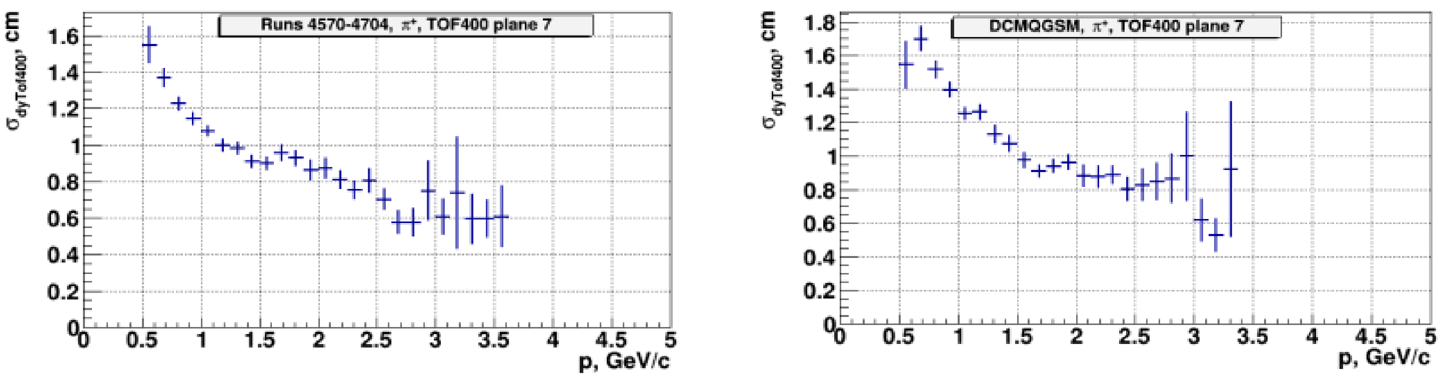

Fig. 7d. Sigma of residuals of *ToF-400* hits in the Y projection with respect to reconstructed positive tracks in dependence on the particle momentum: left plot – experimental data, right plot – simulated tracks.

Mean values of residuals of *DCH* hits

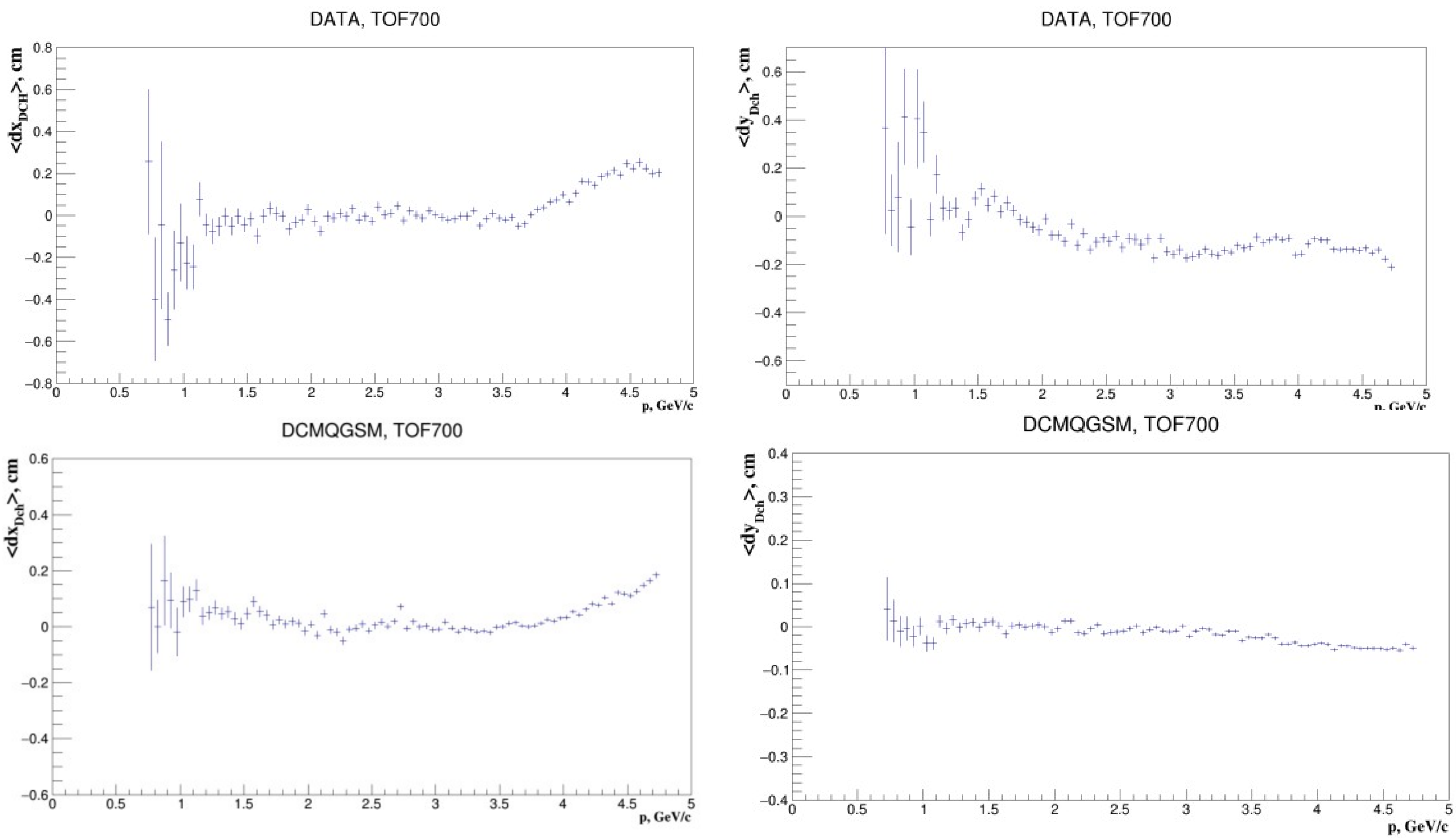

Fig. 8a. *ToF-700* data and simulation: Mean values of residuals of *DCH* hits in X and Y projections with respect to reconstructed positive tracks in dependence on the particle momentum: upper plots experimental data, lower plots – simulated tracks.

Sigma of residuals of *DCH* hits

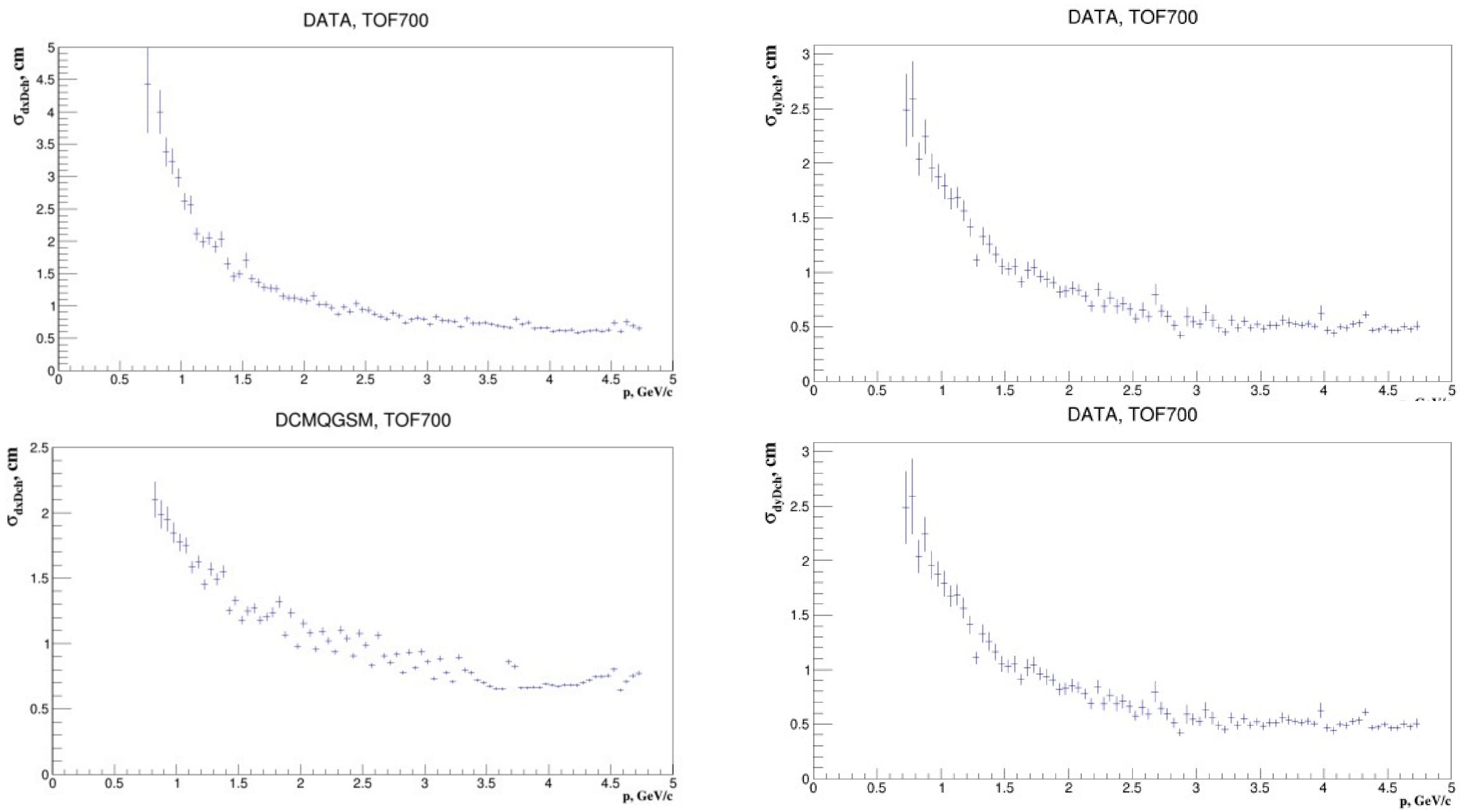

Fig. 8b. *ToF-700* data and simulation: Sigma of residuals of *DCH* hits in X and Y projections with respect to reconstructed positive tracks in dependence on the particle momentum: upper plots experimental data, lower plots – simulated tracks.

Mean values of residuals of *ToF-700* hits

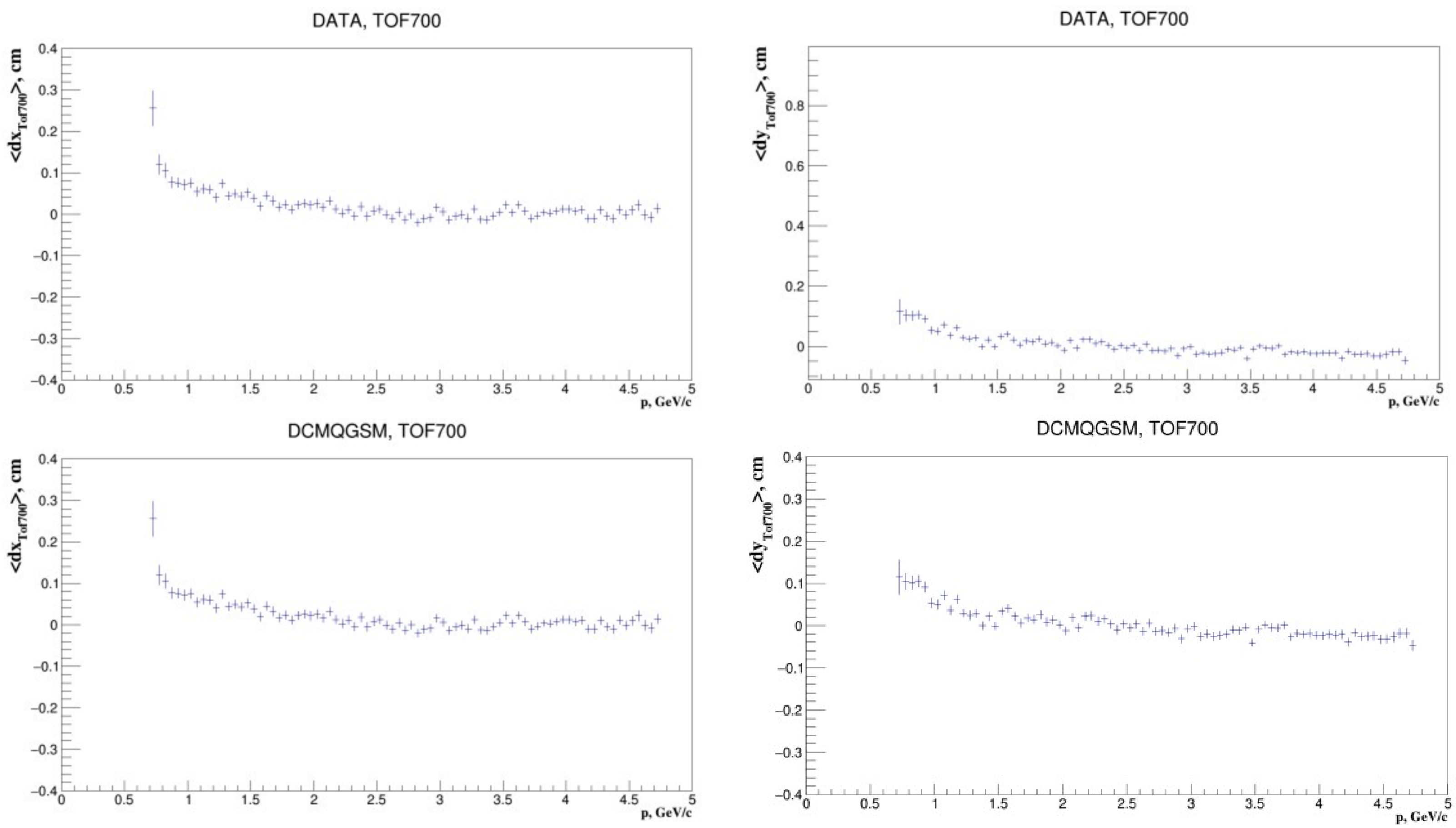

Fig. 9a. Mean values of residuals of *ToF-700* hits in the X and Y projections with respect to reconstructed positive tracks in dependence on the particle momentum: upper plots - experimental data, lower plots - simulated tracks.

Sigma of residuals of *ToF-700* hits

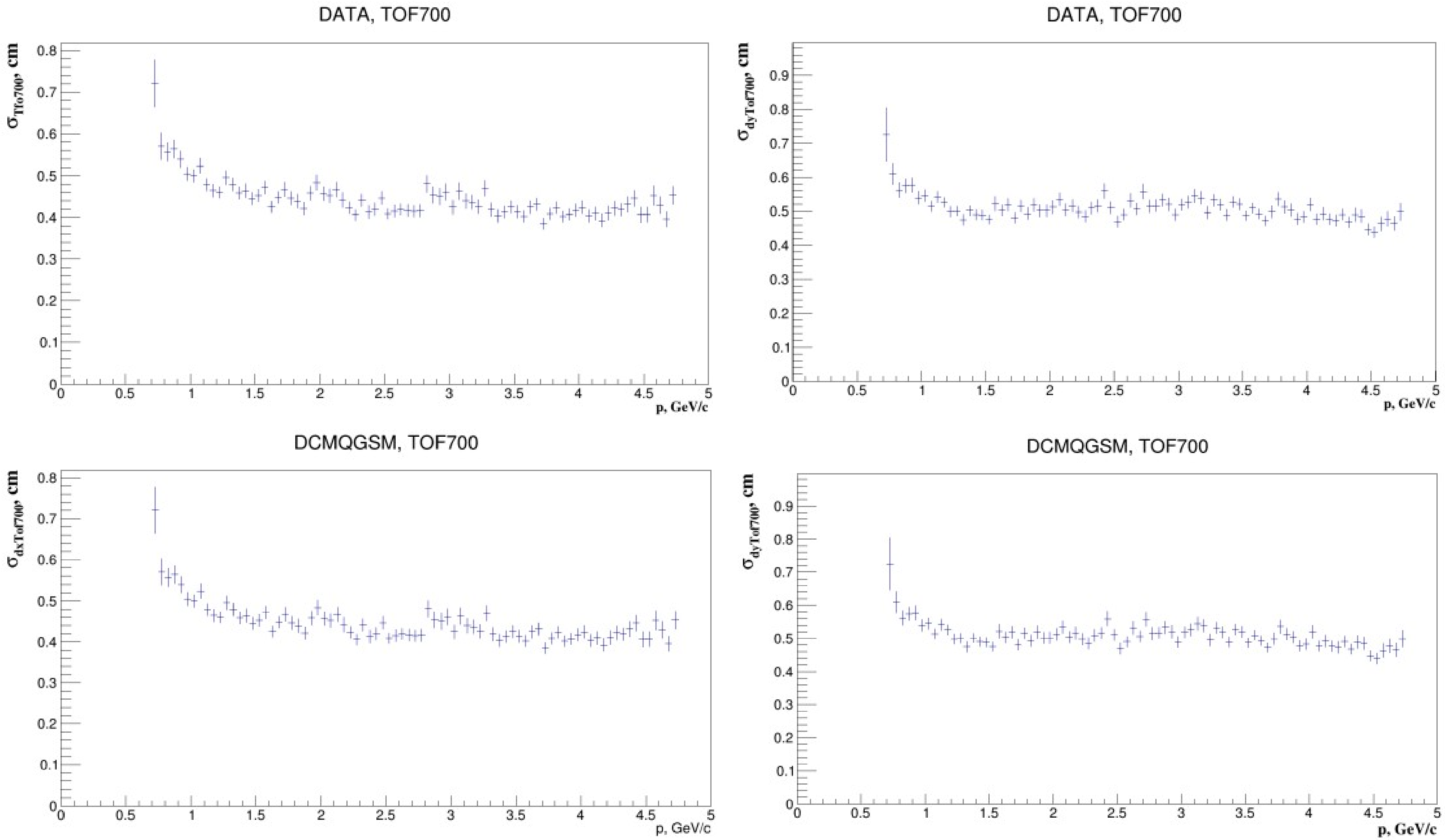

Fig. 9b. Sigma of residuals of *ToF-700* hits in the X and Y projections with respect to reconstructed positive tracks in dependence on the particle momentum: upper plots - experimental data, lower plots - simulated tracks.

n_π/A_{part}

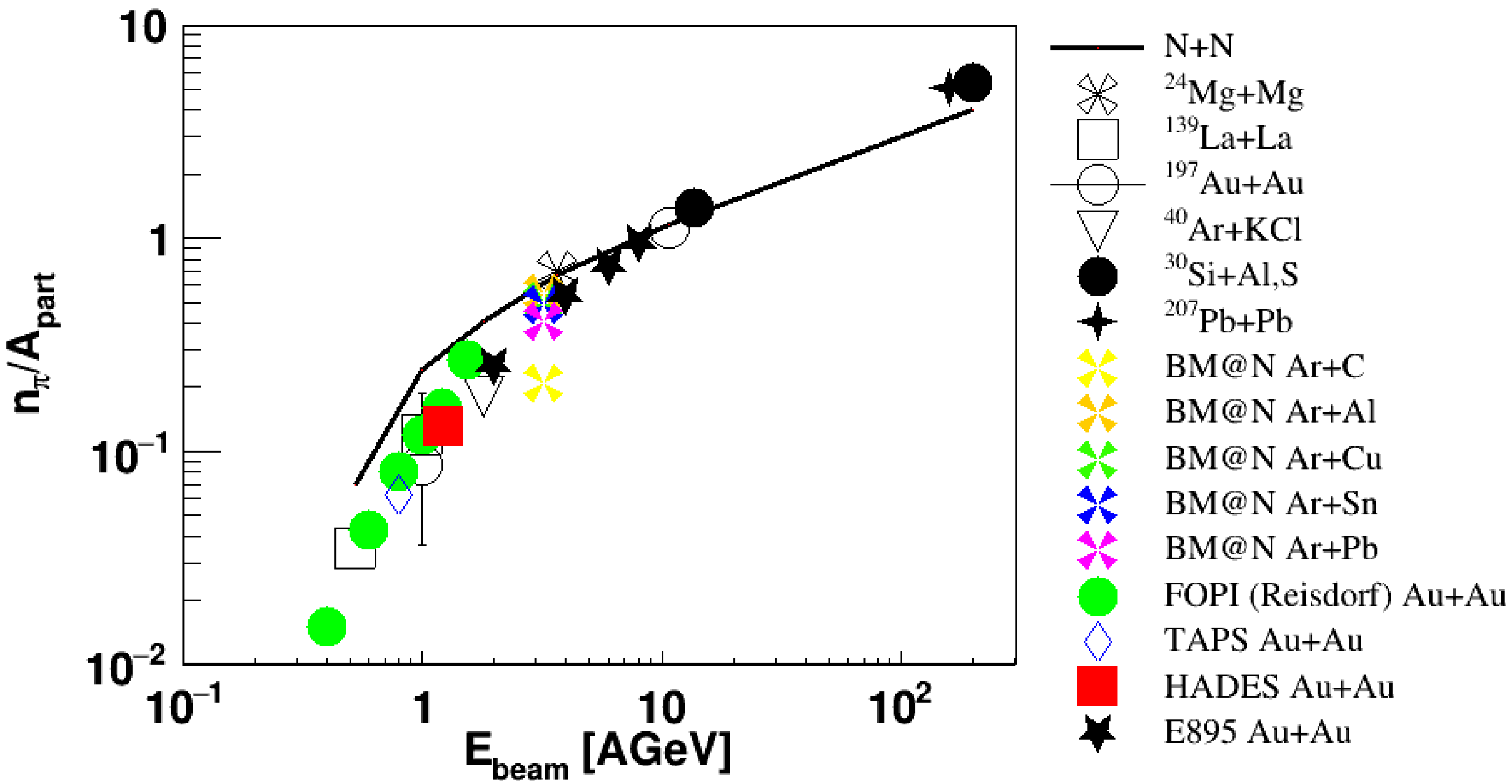

Fig. NNN. Pion multiplicity n_π per mean number of participating nucleon A_{part} as a function of the kinetic beam energy E_{beam}.